POROUS LAYER OPEN TUBULAR COLUMNS WITH IMMOBILIZED TRYPSIN FOR PROTEIN DIGESTION

RADIM KNOB[a], JANA KŘENKOVÁ[b], JAN PETR[a], and FRANTIŠEK FORET[b]

[a] *Department of Analytical Chemistry, Palacký University in Olomouc, Olomouc,* [b] *Institute of Analytical Chemistry, v.v.i., Brno, Czech Republic*
rknob@seznam.cz

Summary

We have developed a monolithic porous layer open tubular (PLOT) column with immobilized trypsin for protein digestion. The PLOT column was prepared in a 10 μm ID fused silica capillary. Trypsin was immobilized on the monolithic surface and the developed enzyme reactor was used for protein digestion followed by on-line ESI/MS analysis.

1. Introduction

Immobilized microfluidic enzyme reactors (IMER) have shown a high potential in a wide variety of research fields such as medical diagnostics, organic synthesis, drug discovery, or biosensors[1,2]. The use of immobilized enzymes, especially of proteases, has many advantages, e.g., very short digestion time, elimination of autodigestion and therefore absence of undesirable protease fragments in the resulting peptide mixture. The reactors with immobilized enzymes can also be integrated online into the multidimensional systems enabling automated high-throughput protein analysis.

A variety of methods are now available for immobilization of enzymes on the solid supports such as particles or monolithic columns[1]. For extremely small sample volumes, the enzymes can be immobilized directly on the wall of very narrow bore capillary (e.g., 10 μm ID or smaller) characterized by a high surface-to-volume (S/V) ratio[3]. The S/V ratio can be further increased by formation of a monolithic porous layer on the capillary wall providing the larger surface area for enzyme immobilization[4].

In this work, we have developed a methacrylate-based PLOT column prepared in a 10 μm ID fused silica capillary. The monolithic surface was modified with trypsin and the developed capillary IMER was coupled on-line to ESI/MS and used for protein digestion.

2. Experimental

2.1. Preparation of the PLOT column

Briefly, a fused silica capillary (Polymicro Technologies, Phoenix, AZ, USA) with the internal diameter of 10 μm was treated with 3-methacryloxypropyl trimethoxysilane[5]. The treated capillary was washed with the polymerization mixture consisting of 24 % (m/m) glycidyl methacrylate, 16 % (m/m) ethylene dimethacrylate, 20 % (m/m) 1-dodecanol, 40 % (m/m) cyclohexanol, 1 % (m/m) azobisisobutyronitrile (AIBN) (with respect to monomers). Then, the capillary was filled with FC-770, a fully fluorinated liquid immiscible with the polymerization mixture[4]. The capillary was sealed with teflon septa and polymerization was performed at 60 °C for 24 hours. After polymerization, the capillary was washed with methanol.

2.2. Trypsin immobilization

The PLOT column was filled with 0.5 mol L^{-1} sulfuric acid and sealed with septa. After 24 hours, the column was washed with water followed by rinsing with a solution of 0.1 mol L^{-1} sodium periodate. TPCK-trypsin (1 mg mL^{-1}) was dissolved in 25 mmol L^{-1} sodium phosphate buffer pH 7.0 containing 3 mg mL^{-1} sodium cyanoborohydride and 0.1 mg mL^{-1} benzamidine. The enzyme solution was pumped through the PLOT column at room temperature for 3 h, washed with the buffer and stored at 4 °C before further use.

2.3. Protein digestion and MS analysis

A solution of bovine cytochrome c (0.1 mg mL^{-1}) was prepared in 10 mmol L^{-1} ammonium bicarbonate pH 7.8 containing 10% acetonitrile and pumped through the reactor at various flow rates using a syringe pump. The digestion was performed at room temperature.

The trypsin reactor was coupled on-line to the Bruker maXis impact ESI-TOF mass spectrometer (Bremen, Germany). The prepared reactor with a polished tip was used as a nanospray needle. The measurements were carried out in the positive ion mode with a scan range of 400–3000 *m*/*z*. The list of detected ions was used for protein identification by the MS-Fit tool of the Protein Prospector database.

3. Results and discussion

A number of different approaches for preparation of PLOT columns have been reported[6]. Most of them rely on

limitation of polymerization kinetics to obtain a polymer layer at the capillary wall; however, inhomogeneity of the thickness is often observed.

Alternatively, the formation of the polymer layer could be restricted to the capillary wall using two immiscible phases. Therefore, the capillary filled with the polymerization mixture was washed with FC-770, a fully fluorinated solvent. This procedure created a thin layer of the polymerization mixture at the capillary wall. A homogeneous PLOT layer was formed by a thermally initiated polymerization of this thin film wetting the capillary wall (Fig. 1).

Trypsin was immobilized on the monolithic surface by a multi-step binding procedure (Fig. 2). First, the epoxide functionalities of the monolith were hydrolyzed by sulfuric acid followed by oxidation using sodium periodate. Trypsin was immobilized via primary amines and the formed Schiff base was stabilized by sodium cyanoborohydride. The enzyme coupling was performed in the presence of benzamidine in order to prevent undesirable autolysis of the enzyme during the immobilization process.

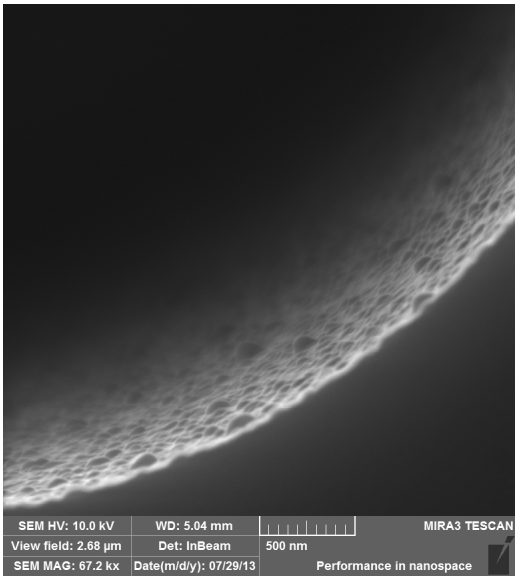

Fig. 1. **Scanning electron micrograph of the PLOT column**

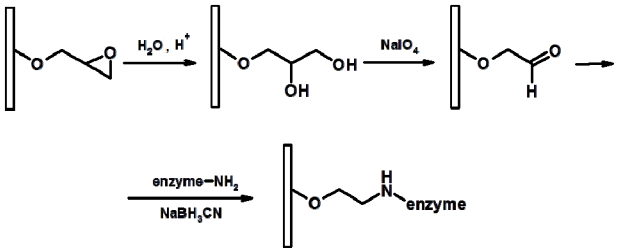

Fig. 2. **Scheme of trypsin immobilization**

Bovine cytochrome c was used as a model protein for digestion using the developed trypsin reactor. The digestion was performed in 10 mmol L^{-1} ammonium bicarbonate pH 7.8 containing 10% acetonitrile in order to minimize non-specific adsorption of protein/peptide on the monolith. The reactor with a polished tip was on-line coupled to the ESI/MS instrument.

The important factor influencing the protein digestion by the trypsin reactor is the protein residence time. Therefore, the protein solution was pumped through the reactor (15 cm, 10 µm ID) at various flow rates (15–100 nL min^{-1}). The corresponding digestion times inside the reactor were 7–50 s. While at the flow rate 15 nL min^{-1} (digestion time: 50 s) the absence of the protein envelope in the mass spectra implied near-complete protein digestion, the appearance of the protein envelope in the mass spectra indicates insufficient digestion at 50 nL min^{-1} (digestion time: 15 s). The sequence coverage obtained with the on-line IMER-MS arrangement was 86.7 % which is comparable with the digestion using soluble trypsin followed by off-line analysis under the same MS conditions (84.8 %).

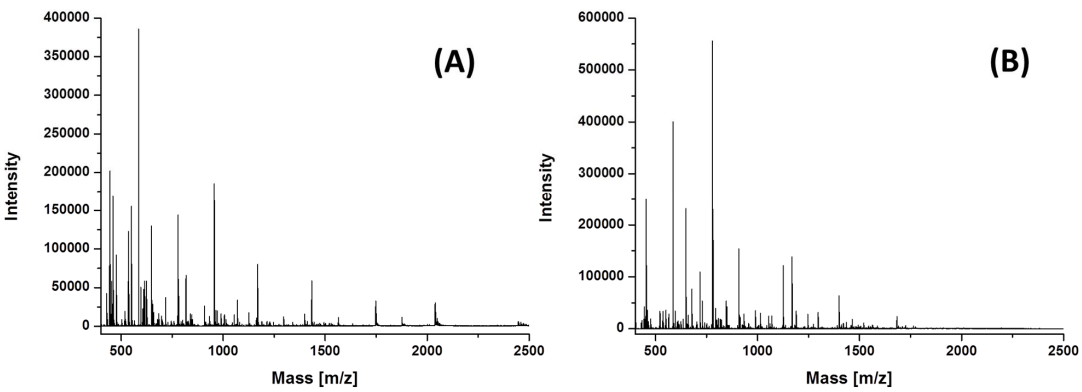

Fig. 3. **Mass spectra of bovine cytochrome c digest.** Digestion time: (A) 15 s, (B) 50 s

4. Conclusions

A monolithic PLOT column with immobilized trypsin for protein digestion was developed. The thin layer PLOT column was prepared using the immiscible phases approach where the formation of the monolith was restricted to the capillary wall by superior wettability of the polymerization mixture after flushing with FC-770. The column was coupled online to ESI/MS and used for digestion of bovine cytochrome c at various flow rates showing near-complete protein digestion in 50 s.

This project was supported by the Operational Programs "Research and Development for Innovations – European Regional Development Fund" (CZ.1.05/2.1.00/03.0058) and "Education for Competitiveness – European Social Fund" (CZ.1.07/2.3.00/20.0018 and CZ.1.07/2.3.00/20.0182). Additional financial support from the Academy of Sciences of the Czech Republic (M200311201) and the institutional research plan (RVO: 68081715) is also acknowledged.

REFERENCES

1. Krenkova J., Foret F.: Electrophoresis *25*, 3550 (2004).
2. Krenkova J., Svec F.: J. Sep. Sci. *32*, 706 (2009).
3. Krenkova J., Kleparnik K., Foret F.: J. Chromatogr., A *1159*, 110 (2007).
4. Knob R., Breadmore M. C., Guijt R. M., Petr J., Macka M.: RSC Advances in press (2013).
5. Rohr T., Hilder E. F., Donovan J. J., Svec F., Frechet J. M. J.: Macromolecules *36*, 1677 (2003).
6. Cheong W. J., Ali F., Kim Y. S., Lee J. W.: J. Chromatogr., A *1308*, 1 (2013).

STUDY OF SEPARABILITY AND DETECTABILITY OF VARIOUS HUMAN INSULIN ANALOGUES AND INSULIN SOLUTION USING RP-HPLC METHOD

VERONIKA KOMOROWSKA and MILAN HUTTA

Department of Analytical Chemistry, Faculty of Natural Sciences, Comenius University in Bratislava, Bratislava, Slovakia
komorowska@fns.uniba.sk

1. Introduction

Human insulin is a peptide hormone consisting of two chains with 21 and 30 amino acids, respectively. These two chains are connected via two disulphide bonds. Its molar mass is 5808 g mol^{-1}. With the latest advances in molecular biology, genomics, proteomics and bioinformatics increased number of biotechnology products which are produced by recombinant techniques. Various recombinant human insulin analogues exist to date. In insulin glulisin two amino acids have been changed in the primary structure. Insulin glargin is characterized by an extension of the B-chain with two additional arginin molecules[1–3]. The various insulin analogues may either show a rapid-acting behavior and are applied directly before the meal or may provide a slow effect which assures a constant basic supply and requires the use one or two times daily.

With the increasing number of these modified analogues, there is a rising need for efficient analysis techniques. A variety of analytical methods, which can be roughly sorted into immunochemical and instrumental analytical methods, had been applied for determination of insulin, e.g.[4]. High performance liquid chromatography (HPLC) is one of the most widely used analytical techniques for the separation of proteins. The aim of our work was initial study of chromatographic behavior of selected recombinant human insulin and its analogues produced by biotechnology process.

2. Experimental

2.1. Chemicals

Formic acid 98–100%, aqueous ammonia 28–30%, methanol (MeOH) 99.9% (v/v), acetonitrile (ACN) 99.9% (v/v), were purchased from Merck (Darmstadt, Germany) all in analytical grade. Samples of human insulin analogues Lantus Solostar (Sanofi Aventis Deutschland GmbH), Apidra (Sanofi Aventis Deutschland GmbH) and sample of regular human insulin Insuman Rapid (Sanofi Aventis, Paris, France), cresol (Lachema, Brno, Czech republic). All aqueous solutions were diluted with ultrapure water purified by Millipore Simplicity (Molsheim, France).

2.2. Chromatography

All chromatographic separations were performed using RP-HPLC C18 column. The HPLC system (Agilent Technologies, Japan) consisted of the following modules: vacuum degasser mobile phases (G1379B), dual-channel high-pressure binary pump (G1312B), auto sampler (G1329B), column thermostat (G1316B), DAD (G1315) and FLD (G1321A). Wavelength range of DAD was set to 190–400 nm. Excitation wavelength FLD was set at 275 nm and emission wavelength at 304 nm. Agilent ChemStation was used for process chromatographic data.

3. Results and discussion

3.1. Study of temperature effect on thermodynamics of separation

For the study were selected temperatures in range from 25 °C to 85 °C and two different organic modifiers (MeOH and ACN) of mobile phase. It is seen from the shown van't Hoff plots in Figs. 1 and 2, that in both types of mobile phases retention behavior of insulin analogues and regular insulin gave nonlinear nature. Nonlinear van't Hoff plots are typical for substances which have a dual retention mechanism, so we can conclude, that for substances under study their complex structure leads to complex interactions in the separation system.

Comparing Figs. 1 and 2, it is clear that the composition of the mobile phase has a considerable influence on the retention behavior of the test compounds at different temperatures. For the separation with a mobile phase consisting of MeOH retention of analytes decreased with increasing column temperature (retention factor varies in the range from 11.34 to 10.83 for insulin glargine, from 11.4 to 11.01 for insulin glulisine and from 11.45 to 10.95 for regular insulin in the temperature range from 25 °C to 85 °C), while the separation with mobile phase consisting of ACN had the opposite trend (retention factor varies in the range from 6.91 to 7.16 for insulin glargine, from 7.00 to 7.37 for glulisine and from 6.99 to 7.31 for regular insulin in the temperature range from 25 °C to 85 °C).

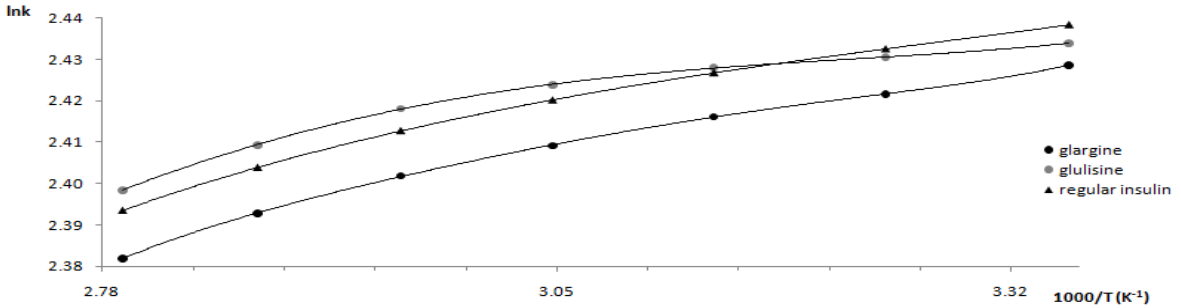

Fig. 1. **Van't Hoff's plot for insulin analogues and regular insulin in mobile phase with MeOH**

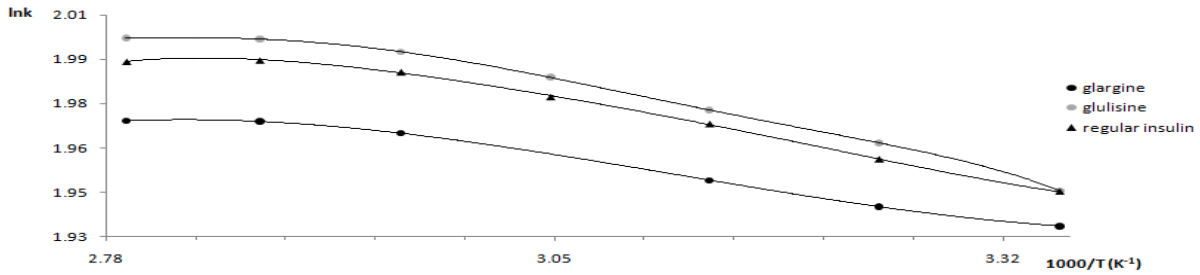

Fig. 2. **Van't Hoff's plot for insulin analogues and regular insulin in mobile phase with ACN**

3.2. Study of organic modifier effect on thermodynamics of sample components separation

Fig. 3 shows that the type of organic modifier has a greater influence on retention of protein nature substance (regular insulin) than on low-molecular weight substance (m-cresol). This result confirms the information given in the literature[5], in which is discussed the fact that an adjustment in thermodynamic conditions of the separation will influence the retention of proteins through changes in the higher protein structures. Therefore it is possible easily influence the selectivity of the separation between the high molecular mass protein substances and low-molecular mass substances with type of organic modifier. The higher selectivity of separation was achieved using MeOH (α = 1.26) than in ACN (α = 1.1).

3.3. Study of detectability of insulin analogues and insulin

For investigation of detectability we used DAD and FLD detector. DAD was set at 280 nm and FLD was set to excitation wavelength at 275 nm and emission wavelength

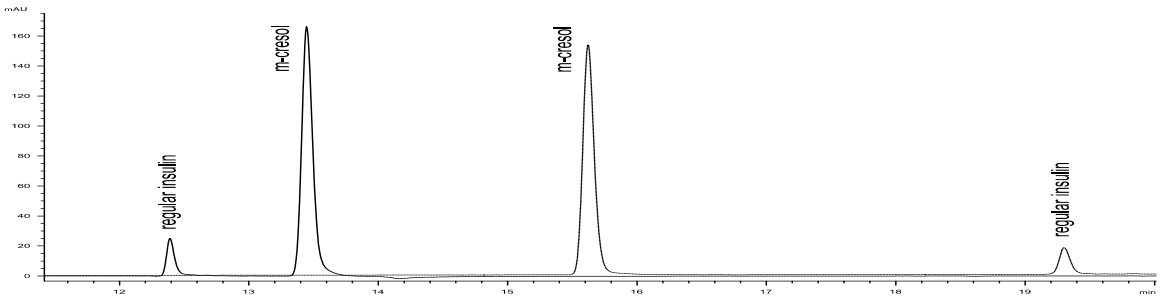

Fig. 3. **Chromatographic results from separation of the sample solution of regular insulin (Insuman Rapid) obtained in two different organic mobile phase modifiers.** Curve with a broken line – the chromatogram obtained with use of MeOH, the curve with the solid line – the chromatogram obtained using ACN. Chromatographic column C18 heated to working temperature (25 °C), the injected volume of sample solutions 50 µL, mobile phase A: buffer from formic acid and amonium formate, mobile phase B: MeOH/H2O (90/10, V/V), appropriate gradient at a flow rate 0.5 mL min^{-1}, UV detection at 280 nm

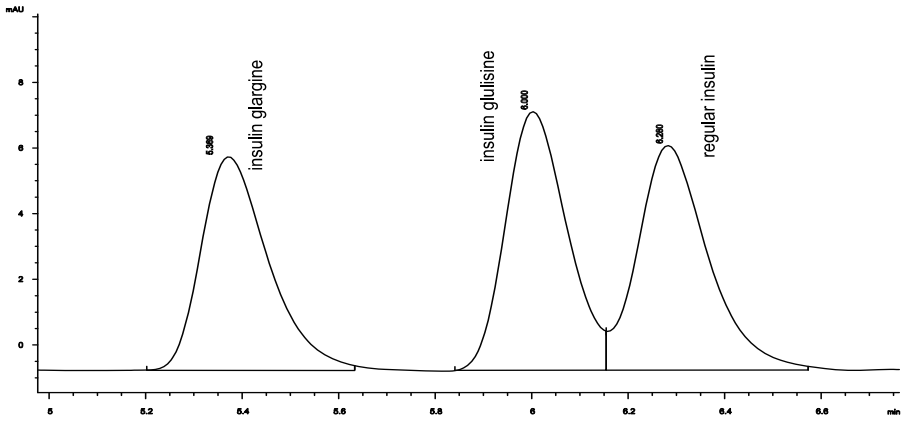

Fig. 4. **Chromatographic results from separation of the mixture insulin analogues and regular insulin.** Chromatographic column C18, the injected volume of sample solutions 50 μL, mobile phase A: buffer from formic acid and amonium formate, mobile phase B: MeOH/H_2O (90/10, V/V), appropriate gradient at a flow rate 0.5 mL min^{-1}, UV detection at 280 nm

at 304 nm. FLD provided better response for all analytes, and thus the lower limits of detection were achieved (data not presented in the paper).

3.4. Separation of mixture insulin analogues and regular insulin

Separation of the mixture was carried out under gradient elution coditions (see Fig. 4). For glargine and human insulin resolution greater than 1.5 was achieved. However, for glulisine and regular human insulin optimization of resolution is still ongoing.

4. Conclusion

In the present work we were able to meet all the objectives of the study. From study we concluded, that there are complex interactions for studied substances even in the RP separation system. With the type of organic modifier of mobile phase is possible significantly affect the selectivity of the separation of the sample components. The higher selectivity was achieved using methanol in the mobile phase. FLD provided better response for the analytes, and thus the lower limit of detection.

This work was generously supported by the grant of project VEGA 1/1349/12 and the grant of project APVV-0583-11.

REFERENCES

1. http://www.drugbank.ca/drugs/DB00030.
2. http://www.drugbank.ca/drugs/DB01309.
3. http://www.drugbank.ca/drugs/DB00047.
4. Ortner K., Buchberger W., Himmelsbach M.: J. Chromatogr., A *1216*, 2953 (2009).
5. Fekete S., Veuthey J. L., Guillarme D.: J. Pharm. Biomed. Anal. *69*, 9 (2012).

UTILIZATION OF LC-MS TECHNIQUES FOR ANALYSIS OF PHENOLIC COMPOUNDS IN VARIOUS TEA SAMPLES

KATARÍNA KRČOVÁ and JOZEF MARÁK

Department of Analytical Chemistry, Faculty of Natural Sciences, Comenius University, Bratislava, Slovak Republic
katarina.krcova@gmail.com

1. Introduction

Phenolic compounds are secondary plant metabolites, which affect organoleptic characteristics of fruits, vegetables and other plants[1,2]. In addition, they show different biological activities such as anti-inflammatory, anti-bacterial, anti-carcinogenic, and play an important role in prevention of osteoporosis and cardiovascular diseases[2–4]. Generally, the term phenolic compounds refers to many different molecules, range from phenolic acids to a complex polyphenols[5]. A plant phenolic compounds posses one or more aromatic or heterocyclic rings, bearing one or more hydroxyl groups[3]. Phenolic compounds are important components mostly present in different sorts of red and white wines, teas, herbals, fruits, vegetables, cereals and spices[1,6,7]. The group of herbal phenols forms: phenolic acids and their derivates, tannins, flavonoids, isoflavonoids, prenylated flavonoids, derivates of coumarin, derivates of stilbene and other phenolic compounds[3]. Tea has been used as an important drink for over 1000 years because of its beneficial effect for the human body. It is one of the most widely consumed soft drinks in the world, next to the water. The content of individual phenolic compounds in tea varieties is highly variable which is caused by using of different fermentation procedure, growing season and different geographical region[8].

The aim of this work was developing and utilization of HPLC-IT-TOF MS method for analysis and identification of phenolic compounds in selected tea samples prepared from various plants, normally grown in the Slovakia (for the list of plants, see Tab. I). The individual plant samples were obtained from Myjava region and the harvesting period was from March to September, 2012.

2. Experimental

2.1. LC-MS analysis

HPLC-MS analyses of selected tea samples prepared from various plants and their phenolic profiles were performed by means of Shimadzu LCMS-IT-TOF™ (Shimadzu, Kyoto, Japan). Chromatographic separations were performed on Kinetex XB-C18 column (100 × 2.1 mm; 2.6 μm) (Phenomenex, Torrance, CA, USA) using gradient elution: water + 0.1% formic acid (A)/ acetonitrile + 0.1% formic acid (B) with 0.2 mL min^{-1} flow rate (0 min: 5% B; 3 min: 10%B; 8 min: 40%B; 10 min: 60% B; 11 min: 90% B; 12 min: 90% B; 12,1 min: 5% B; 20 min: 5% B). The column was thermostated to 40 °C. The MS1-MS3 analyses were performed in automatic data acquisition mode within 50–1000 *m/z* range in both positive and negative ionization modes and within 190–400 nm wavelengths used in DAD detection. Data acquisition and data evaluation were performed by using LCMS Solution ver. 3.51 (Shimadzu). Total analysis time was 20 minutes and injected volumes were 2 μL or 5 μL, respectively.

2.2. Chemicals

Chemicals used in this work were obtained from Merck (Merck, Darmstadt, Germany) and Sigma-Aldrich (Sigma-Aldrich, Steinheim, Germany) in analytical grade purity. Acetonitrile and water (both LC-MS purity) were purchased from Merck. Formic acid (LC-MS purity) was purchased from Sigma-Aldrich.

2.3. Samples

22 plant samples analyzed in this work (see Tab. I) were obtained from Myjava region (Slovak republic), with harvesting period March – September 2012. Consequently, the individual samples were dried and stored in cool and dry place. The tea extracts were prepared as follows: Approximately 2.0 g (for accurate weights of individual samples, see Tab. I) of dried sample was extracted with 100 mL of boiling water. Extraction time was 15 minutes. In the following step, the extracts were filtered through 0.8 μm syringe micro filter and cooled to laboratory temperature before their HPLC-MS analyses.

3. Results and discussion

The first part of this work was to find the optimal conditions for chromatographic separation of phenolic compounds in selected tea samples from various plants. Consequently, the mass-spectrometric detection of selected tea samples was performed. Total analysis time was 20 minutes. 22 samples prepared from various plants (see Tab. I) were obtained from Myjava region (Slovak republic). MSXelerator software version 2.4 was used for the visualization of obtained data. Obtained

Table I
Selected tea samples of various plants analyzed in this work

No.	Name of Plant	Name of Plant (Latin)	Mass [g]	Picking period	Analyzed part of plant
1	Breckland Thyme	Thymus serpyllum	2.01	06/2012	blossom, leaves, stem
2	Sage	Salvia officinalis	2.01	06, 07/2012	leaves, stem
3	Common Agrimony	Agrimonia eupatoria	2.00	07/2012	leaves, stem, haulm
4	Lemon Balm	Melissa officinalis	2.00	06, 07/2012	leaves, stem
5	Pot Marigold	Calendula officinalis	2.00	06-09/2012	blossom
6	Eyebright	Euphrasia rostkoviana	1.99	07, 08/2012	haulm, leaves, stalk
7	Chamomile	Matricaria chamomilla	2.00	06/2012	blossom, stem
8	Ribwort Plantain	Plantago lanceolata	2.00	05-08/2012	leaves
9	Lady`s Manthle	Alchemilka xanthochlora	2.02	07, 08/2012	blossom, leaves, stem
10	Garden Thyme	Thymus vulgaris	2.00	07-09/2012	blossom, haulm, stem
11	Coltsfoot	Tussilago farfara	1.99	04/2012	blossom
12	Common Centaury	Centaurium minus	2.02	06-09/2012	leaves, stem, haulm
13	Woodland Strawberry	Fragaria vesca	1.95	05, 06/2012	blossom, leaves, stem
14	Parsley	Petroselinum crispum	2.01	07/2012	haulm
15	Lavender	Lavandula officinalis	1.98	06-08/2012	blossom, leaves, stem
16	Field Horsetail	Equisetum arvense	2.02	06-09/2012	haulm
17	Elderberry	Sambucus nigra	2.00	05/2012	blossom, stem
18	Stinging Nettle	Urtica dioica	1.99	06-09/2012	leaves
19	Lungwort	Pulmonaria officinalis	1.98	03-05/2012	leaves, stem, haulm
20	Yarrow	Achillea millefolium	2.00	07, 08/2012	blossom, stem
21	Cowslip	Primula veris	1.99	03, 04/2012	blossom
22	Small-leaved Lime	Tilia cordata	2.00	06, 07/2012	blossom

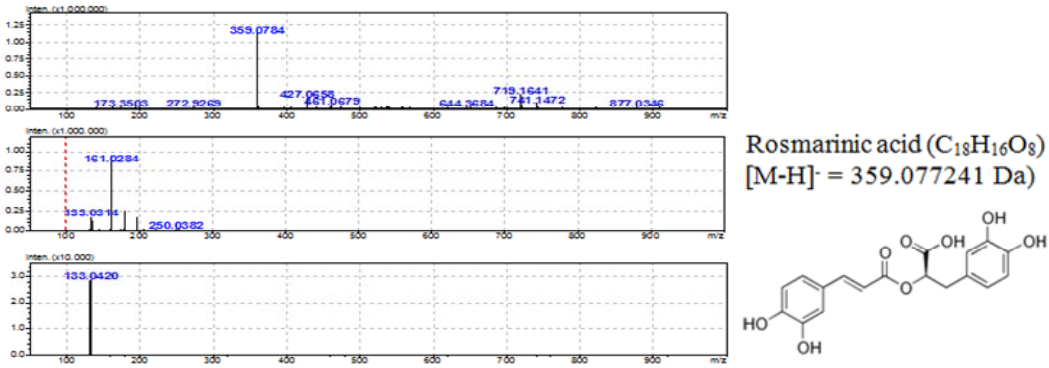

Fig. 1. **TIC and EIC traces obtained from HPLC-MS analysis of 2 µL of tea extract from Melissa officinalis**

chromatograms and MS spectra show the different composition of individual tea samples and their different phenolic profiles. (Fig. 1, Fig. 2).

4. Conclusions

The aim of this work was the development of the suitable method based on the combination high performance liquid chromatography and mass spectrometry and its utilizing for the characterization and

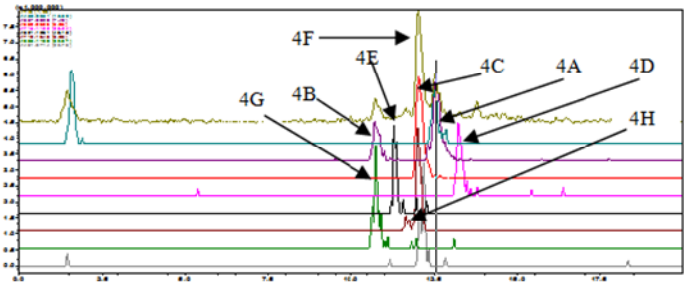

No.	Phenolic compound
4A	Sulphated rosmarinic acid
4B	Lithospermic acid A isomer
4C	Rosmarinic acid
4D	Salvianolic acid C derivate
4E	Rosmarinic acid hexoside
4F	Sagerinic acid
4G	Salvianolic acid K derivate
4H	Luteolin-3'-O-glucuronide

Fig. 2. **MS3 spectra of identified phenolic compound - Rosmarinic acid in extract from Melissa officinalis**

identification of several phenolic compounds present in tea samples prepared from various plants (see Tab. I) obtained from Myjava region. Identified phenolic compounds in extracts from Melissa officinalis are shown on Fig. 2.

This work was financially supported by Slovak Research and Development Agency (Project VVCE-0070-07, APVV-0583-11), Slovak Grant Agency (project No. VEGA 1/1305/12) and Grant UK (UK/608/2013).

REFERENCES

1. Ignat I., Volf, I., Popa V. I.: Food Chem. *126*, 1821 (2011).
2. Boros B., Jakabova S., Dornyei A., Horvath G., Pluhar Z., Kilar F., Felinger A.: J. Chromatogr., A *1217*, 7972 (2010).
3. [Cited: 4. September 2013] < http://web.vscht.cz/koplikr/Rostlinnefenolya flavonoidy.pdf >
4. Ginjom I., D'Arcy B., Caffin N., Gidley M.: Food Chem. *125*, 823 (2011).
5. Jaitz L., Siegl K., Eder R., Rak G., Abranko L., Koellensperger G., Hann S.: Food Chem. *122*, 366 (2010).
6. [Cited: 1. June 2013]<http://referaty.atlas.sk/prirodnevedy/chemia/50908/?pri nt=1>
7. Atoui A. K., Mansouri A., Boskou G., Kefalas P.: Food Chem. *89*, 27 (2005).
8. Zhao Z., Chen P., Lin L., Harnly J. M., Yu L. L., Li Z.: Food Chem. *126* 1269 (2011).

IEF AND HPLC-BASED METHODS FOR EFFICIENT BACTERIAL CHARACTERIZATION

ANNA KUBESOVÁ, JIŘÍ ŠALPLACHTA, DANA MORAVCOVÁ, and MARIE HORKÁ

Institute of Analytical Chemistry of the ASCR, v. v. i., Veveří 97, 602 00 Brno, Czech Republic
kubesova@iach.cz

Summary

Pectobacterium and *Dickeya* species are responsible for blackleg and tuber soft rot diseases on crop and ornamental plants. Recently, a more virulent and aggressive *Dickeya* type of *E. chrysanthemi* was described and it becomes serious problem for potato production in Europe. In this study, we suggest procedures using two commonly available laboratory techniques, gel isoelectric focusing and liquid chromatography, for differentiation and characterization of *Pectobacterium* and *Dickeya* species. We have confirmed that fingerprinting approach can be used for bacterial differentiation, which can be further used in rapid diagnosis of plant disease.

1. Introduction

Bacteria of the genus *Dickeya* cause blackleg and soft rot disease of many plants[1–4]. Recently, *Dickeya* spp. have become serious problem for potato production in Europe. In 2005, new type of *E. chrysanthemi*, was described and named as *Dickeya solani.* This new type is more aggressive than the other *Dickeya* spp.[4,5].

The aim of this study was to discriminate different *Pectobacterium* and *Dickeya* spp., including *D. solani*, using gel isoelectric focusing (IEF) and high performance liquid chromatography (HPLC).

2. Experimental

2.1. Plant pathogens

Strains of *Pectobacterium* and *Dickeya* spp. were obtained from three different collections: La ollection Française de Bactéries associées aux Plantes, Angers, France (CFBP); Plant Research International, Wageningen, Netherlands (PRI); and Czech Collection of Microorganisms, Brno, Czech Republic (CCM).

2.2. Sample preparation

IEF and HPLC were carried out with proteins precipitated from particular cell lysates. Cell lysates were prepared by incubation of bacterial cell suspensions in 8% (w/v) Brij 35 and 20% (v/v) EtOH (ref.[6]). The suspension containing10^{10} cells mL^{-1} was incubated at 30 °C for 16 h. The resulting supernatant was acquired after 60 min of centrifugation at 6000 g on MiniSpin (Eppendorf AG, Hamburg, Germany). The acetone precipitation procedure was used to get proteins from the individual cell lysates.

2.3. IEF

Gel IEF was carried out using apparatus 111 Mini IEF Cell (Bio-Rad) at the pH gradient 3–10 formed by carrier ampholytes. The p*I* markers, 2.0, 3.1, 4.3, 5.3, 6.3, 7.1, 8.0, 9.0, 9.8 (concentration of individual p*I* markers was 1 mg mL^{-1}), and 6 μL of the bacterial sample were loaded onto the gel. The power supply VNZ 22 (Developmental manufactories of ČSAV, Praha, Czech Republic) was used for running of the gel at constant power of 0.6 W, voltage limit 400 V. Brij 35 (0.08% (w/v)) was added into the gel for better solubility of the analyzed proteins[6]. Protein visualization was carried out with CBB G-250 in accordance with manufacturer`s manual. Image of the stained gel was acquired by UMAX Astra 3400 scanner (UMAX Technologies, Dallas, TX, USA) and the gel image was processed using Quantity One Quantification Software (ver. 4.6.0, Bio-Rad).

2.4. HPLC

HPLC experiments were carried out using an Agilent 1200 Series chromatographic system (Agilent Technologies, Santa Clara, CA). Separations were performed on a microbore Poroshell 300SB-C18 column (5-μm particle size, 1 × 75 mm, Agilent Technologies) equipped with a C18 cartridge guard. The elution was run at a flow rate of 20 μL min^{-1} and 70 °C by a binary gradient with acetonitrile as an organic modifier. Solvent A consisted of 0.1 % (v/v) TFA in water and solvent B contained 0.1 % (v/v) TFA in acetonitrile. The used gradient profile consisted of isocratic step (5% solvent B in A) over 5 min and linear gradient elution from 5 to 70 % (v/v) B over 30 min. The detection was performed at 214 nm using a diode-array detector.

3. Results and discussion

A total of 42 strains of *Pectobacterium* and *Dickeya* spp. were subjected to IEF and HPLC analyses. With respect to IEF, each bacterial species provided characteristic protein fingerprint and shows feasibility of the suggested IEF method for reliable characterization and differentiation of the bacteria. These species differ in the p*I* values of the detected protein zones mainly in the p*I* range 4.5–8.0. The samples processed in the same way as

for IEF were further analyzed by HPLC using gradient elution. Under optimized experimental conditions, each individual species owns a unique protein fingerprint. Obtained data shows that this technique is capable to differentiate examined bacteria at the species level as well.

4. Conclusions

Fingerprinting approaches using gel IEF and HPLC have proved effective tools for bacterial differentiation, where the unique IEF patterns or characteristic elution profiles (HPLC) can be used to identify different bacterial species.

This work was supported by the Ministry of the Interior of the Czech Republic (Grant VG20102015023 and Grant VG20112015021) and by the Academy of Sciences of the Czech Republic (Institutional Support RVO:68081715).

REFERENCES

1. Samson R., Legendre J. B., Christen R., Fishcer-Le Saux M., Achouak W., Gardan L.: Int. J. Syst. Evol. Microbiol. *55*, 1415 (2005).
2. Tsror (Lahkim) L., Erlich O., Lebiush S., Zig U., van de Haar J.: Proceedings of the 11th International Conference on Plant Pathogenic Bacteria, 2006, Edinburgh, Scotland, 70.
3. Tsror (Lahkim) L., Erlich O., Lebiush S., Hazanovsky M., Zig U., Slawiak M., Grabe G., van der Wolf J. M., van de Haar J. J.: Eur. J. Plant Pathol. *123*, 311 (2009).
4. Toth I. K., van der Wolf J. M., Saddler G., Lojkowska E., Helias V., Pirhonen M. L., Elphinstone J. G.: Plant Pathology *60*, 385 (2011).
5. Sławiak M., Beckhoven J. R. C. M., Speksnijder A. G. C. L., Czajkowski R., Grabe G., van der Wolf J. M.: Eur. J. Plant Pathol. *125*, 245 (2009).
6. Horká M., Růžička F., Holá V., Šlais K.: Electrophoresis *30*, 2134 (2009).

CONTRIBUTION OF HEVYLITE ASSAYS BY PATIENTS WITH MONOCLONAL GAMMOPATHY

PAVLÍNA KUŠNIEROVÁ[a,b], DAVID ZEMAN[a,b], RADKA ŠIGUTOVÁ[a,b,c], VĚRA PLOTICOVÁ[a,b], FRANTIŠEK VŠIANSKÝ[a], and ZDENĚK ŠVAGERA[a,b]

[a] *Department of Clinical Biochemistry, Institute of Laboratory Diagnostics, University Hospital Ostrava, Ostrava,* [b] *Department of Biomedical Sciences, Faculty of Medicine, University of Ostrava, Ostrava,* [c] *Department of Biochemistry, Faculty of Medicine, Masaryk University, Brno, Czech Republic*
pavlina.kusnierova@fno.cz

1. Introduction

Identification of monoclonal gammopathy is based on protein electrophoresis of serum and urine as well as on the quantification of free kappa and lambda light chains[1]. For detection of monoclonal gammopathy, the levels of immunoglobulin heavy/light chains pairs (Hevylite™) have recently become important[2].

Immunoglobulin heavy chain/light chains assay (Hevylite™) is a new analytical method. It uses specific sheep polyclonal antibodies against junctional epitopes between domains of heavy and light chain in the constant region of immunoglobulin chains[2]. This method enables the individual determinations of the concentrations of k and λ light chains in the intact molecule IgG, IgA, IgM types of monoclonal immunoglobulin. The ratio of Igκ/Igλ is also used as an "index of clonality". This methodology is also independent of the state of renal clearance and variability of blood volume and reflects suppression of non-tumor Ig (ref.[3]). The ratio of Igκ/Igλ provides quick and dynamic information about the degree of therapeutic effect and may be helpful for monitoring the progress of disease. Long-term monitoring of changes in Igκ/Igλ should serve to capture incomplete remission of multiple myeloma (already determined as a negative finding on immunofixation but still exhibiting an abnormal ratio), to detect an incomplete therapeutic effect, and to detect an early stage of relapse (pathological values of Igκ/Igλ appear considerably sooner than positivity of IFE). This method has greater sensitivity with a higher range of measured values and enables accurate diagnosis of unsatisfactory or absent therapeutic effect of chemotherapy. What is more, it has the potential for earlier detection of relapse or disease progression in comparison with electrophoretic monitoring of serum monoclonal immunoglobulin with immunofixation results. In patients with AL amyloidosis, the results of studies also indicated high sensitivity of this method in patients with low levels of monoclonal immunoglobulin. This method could therefore be used for monitoring the effect of treatment in cases which present a normal result in an examination of free light chains in serum. This method could be useful in cases where assessment of disease progression and effectiveness of treatments is difficult to determine[2,4–7]. Studies on malignant lymphoproliferative diseases and the Igκ/Igλ ratio showed higher sensitivity of the method in comparison with conventional electrophoresis in patients with non-Hodgkin lymphoma (48 %), primary macroglobulinemia (100 %), diffuse B-cell lymphoma (65 %), mantle cell lymphoma (63 %), and follicular lymphoma (29 %) (ref.[8]).

2. Experimental

We examined a group of 67 patients suspected of monoclonal gammopathy. The first sample included 27 patients with monoclonal immunoglobulin IgG, the second sample consisted of 23 patients with monoclonal immunoglobulin IgA, and the third group consisted of 17 patients with monoclonal immunoglobulin IgM. Patients were monitored for the following laboratory parameters in serum: total protein and albumin (spectrophotometry, AU 5400, Beckman Coulter, Brea, CA, USA), immunoglobulins G, A, M (nephelometry, BN ProSpec, Siemens Healthcare Diagnostics Inc., Newark, DE, USA), free light chains and light chains kappa and lambda in the intact Ig molecule (turbidimetry, SPA Plus, The Binding Site Group Ltd, Birmingham, UK), serum protein electrophoresis and immunofixation electrophoresis (Hydrasys, Sebia Benelux S.A., Brussels, Belgium). Densitometric values were obtained using a scanner EPSON Perfection V700 Photo and Phoresis software version 7.4.7. (A. L. Instruments, s.r.o., Czech Republic). Statistical evaluation of results was performed using MedCalc software version 11.4 (Frank Schoonjans, Belgium).

3. Results and discussion

We examined the relationship between the densitometrically observed value of monoclonal immunoglobulin and the concentration of light chains kappa or lambda in the intact immunoglobulin molecule (Hevylite™) obtained by the turbidimetric assay. With regard to the non-normal distribution of measured data, the results of analysis were evaluated by Spearman's correlation coefficient "Rho" (r_s) and Kendall´s "Tau" correlation coefficient (r_τ) (Tab. Ia–Ib). The higher values

Table Ia
Results of rank correlations of monoclonal IgG: the densitometrically observed value of monoclonal immunoglobulin vs. the concentration of Hevylite; and total IgG vs. summation of the respective Hevylite pair. Correlations were determined using Spearman's Rho values and Kendall's Tau values

	DM value vs. IgGκ	DM value vs. IgGλ	IgG vs. IgGκ+IgGλ
n	21	6	27
Spearman´s Rho	0.87 p<0.0001	0.94 p=0.0048	0.93 p<0.0001
Kendall´s Tau	0.68 p<0.0001	0.87 p=0.0242	0.77 p<0.0001

Table Ib
Results of rank correlations of monoclonal IgA/IgM: the densitometrically observed value of monoclonal immunoglobulin vs. the concentration of Hevylite; and total IgA/IgM vs. summation of the respective Hevylite pair. Correlations were determined using Spearman's Rho values and Kendall's Tau values

	DM value vs. IgAλ	DM value vs. IgAκ	IgA vs. IgAκ+IgAλ	DM value vs. IgMκ	IgM vs. IgMκ+IgMλ
n	16	7	31	14	14
Spearman´s Rho	0.76 p=0.0007	0.96 p=0.0005	0.95 p<0.0001	0.94 p<0.0001	0.99 p<0.0001
Kendall´s Tau	0.63 p=0.0007	0.91 p=0.0069	0.85 p<0.0001	0.84 p<0.0001	0.96 p<0.0001

Table II
Determination of regression equations (y = a + b×x) for the concentration of IgG and the sum of respective Hevylite pair and for the concentraction of HLC and DM value

x	IgGκ+IgGλ	IgGκ	IgGλ
y	IgG	DM value	DM value
n	27	21	6
Coefficient of determination	0.81	0.79	0.75
Regression equation	y=1.66+1.07·x	y= -3.05+0.97·x	y=1.27+0.69·x

of both correlation coefficients were found between concentrations of IgA kappa (Hevylite™) and the densitometric value of monoclonal immunoglobulin IgA kappa (r_s=0.964 and r_τ=0.905) (Tab. Ib). The lower values of both correlation coefficients were found between IgA lambda vs. DM value (r_s=0.756, r_τ=0.633) (Tab. Ib). Correlation between DM value and IgM lambda was not evaluated because of the small amount of data. The same procedure was used when evaluating correlations between the concentration of the particular immunoglobulin measured by the nephelometry and the sum of the concentrations of kappa and lambda light chains in the intact immunoglobulin molecule (Hevylite™) obtained by the turbidimetry assay. The highest correlation was found in the monoclonal protein IgM (r_S=0.991, P<0.0001; r_T=0.956, P<0.0001). The same correlation was found in the remaining two groups (Tab. Ib).

The regression analysis shows that over 90 % of the measured values were explained by the regression relationship. The highest agreement in the group with M-

Table III
Determination of regression equations (y = a + b×x) for the concentration of IgM and IgA and the sum of respective Hevylite pair and for the concentraction of HLC and DM value

x	IgMκ+IgMλ	IgMκ	IgAκ+IgAλ	IgAκ	IgAλ
y	IgM	DM value	IgA	DM value	DM value
n	14	14	31	7	16
Coefficient of determination	0.94	0.86	0.94	0.95	0.53
Regression equation	y=0.48+0.72·x	y=1.71+0.37·x	y=3.03+0.66·x	y=–0.74+0.60·x	y=0.32+0.66·x

protein IgG was found between the concentration of IgG and the sum of IgGκ+IgGλ (r^2=0.81) and the lowest agreement between the concentration of IgG lambda and DM value (r^2=0.75), (Tab. II). In the group with the M-protein of the monoclonal IgM, we again observed very good agreement between the concentration of IgM and the sum of IgMκ+IgMλ (r^2=0.94), (Tab. III). The tightness of fit to the regression line expressed by the coefficient of determination was practically the same in M-protein IgA kappa vs. DM value and the concentration of monoclonal IgA vs. the sum of the concentrations IgAκ +IgAλ (r^2=0.943 and 0.947), (Tab. III). In contrast, the tightness of fit of the measured points by the regression line of M-protein IgA lambda was low (r^2=0.528), (Tab. III).

4. Conclusions

Methods for the determination of free light chains and kappa or lambda light chains in the intact molecule of Ig (HevyliteTM) complement the routine examinations of patients with monoclonal gammopathy, but they cannot replace the routine examination at all. The HLC method appears to be particularly useful in quantifying monoclonal immunoglobulin of the IgA classes. The region of their electrophoretic migration is often at the same site of migration of beta-globulins, causing "overlapping" of M-proteins. The differences between the values determined by HLC, total Ig concentration and densitometrically determined values of M protein may be attributed to the problem of maximum saturation of agarose gel. Furthermore, variations can be induced by the type of dye used and by the differences in reactivity caused by the use of reagents with variable antibody specificity.

REFERENCES

1. Bird J. M., Owen R. G., DęSa S., et al.: Brit. J. Haematol. *154*, 32 (2011).
2. Bradwell A. R., Harding S. J., Fourrier N. J., Wallis G. L. F., Drayson M. T., Carr-Smith H. D., Mead G. P.: Clin. Chem. *55*, 1646 (2009).
3. Alexanian R.: Blood *49*, 301 (1977).
4. Keren D. F.: Clin. Chem. *55*, 1606 (2009).
5. Ludwig H., Harding S., Bradley C., Milosavljevich D., Drayson M., Morgan G., et al.: Blood *114*, (abstract 4879) (2009).
6. Wechalekar A., Harding S., Lachmann H., Gillmore J. D., Wassef N. L., Thomas M., et al.: Amyloid-Journal of protein folding disorders *17*, 188 (2010).
7. Donato L. J., Zeldenrust S. R., Murray D. L., Katzmann J. A.: Clin. Chem. *57*, 1645 (2011).
8. Bradwell A. R., in: (Bradwell A. R.) *Serum Free Light Chain Analysis (plus Hevylite),* Sixth Edition, p. 301–320. Birmingham: The Binding Site Ltd 2010.

KINETIC CHARACTERIZATION OF CYTOCHROME P450 2C9 HYDROXYLATION OF DICLOFENAC BY CAPILLARY ELECTROPHORESIS – MASS SPECTROMETRY

MONIKA LANGMAJEROVÁ, ROMAN ŘEMÍNEK, and ZDENĚK GLATZ

Department of Biochemistry, Faculty of Science and CEITEC – Central European Institute of Technology, Masaryk University, Brno, Czech Republic
langmajerova@ceitec.muni.cz

Summary

The automatized method comprising injection of substrates, incubation, separation of reaction products by CE and their identification and quantification by Qq-TOF mass spectrometry (MS) was successfully used for kinetic measurements of enzymatic reaction. Enzymatic system consisting of cytochrome P450 izoform 2C9 (CYP2C9) and diclofenac (DC) provided these apparent kinetic values: K_m' 4.7 μM and V_{max}' 1.1 nmol min^{-1} nmol^{-1} CYP2C9.

1. Introduction

Cytochrome P450 enzymes represent one of the most important systems involved in drug metabolism[1]. The interactions between these enzymes and drugs are defined by reaction kinetics and drug-drug interactions etc.[2]. An automated system integrating the mixing of reactants, the incubation and the subsequent separation and detection can be advantageously used for such extensive screenings. There are two approaches for CE assay. Off-line CE assay is generally performed in two steps, when a reaction mixture is incubated in the vial and then analyzed by CE. On the contrary the on-line CE assay exploits space inside the capillary as a reaction chamber and as a separation column as well. Moreover, CE combined with MS/MS detection allows target identification and its quantification.

2. Experimental

2.1. Capillary electrophoresis

Analyses were performed on Agilent 7100 CE System. Bare fused-silica capillary (75 cm length, 75 μm i.d., 363 μm o.d.) filled with 30 mM ammonium acetate (pH 8.7) as BGE was used. Separation was carried out by application of voltage –22 kV (293 V/cm) at 37 °C. Linear voltage gradient from 0 kV to –22 kV during first 0.2 min and positive pressure 100 mbar after 6.5 min of analysis was applied.

2.2. On-line reaction

Solutions of CYP2C9 enzyme (E) and mixture of substrate and cofactor (S) dissolved in incubation buffer were injected hydrodynamically by pressure 15 mbar into capillary according previous published work[3] – S solution for 3, 3, 3 and 6 s and E solution three times for 3 s between S plugs. Resulting reaction mixture contained 17.5 nM CYP2C9, 1 mM NADPH and required concentration of DC. Incubation was performed for 10 minutes and the reaction was terminated by voltage application. All steps are visualized by Fig. 1.

2.3. Mass spectrometry

Bruker maXis impact quadrupole time-of-flight MS was coupled to CE. The connection was enabled by sheath liquid co-axial interface from Agilent and sheath liquid (ShL) containing 0.5% ammonia dissolved in isopropanole-water (1:1, v/v) was delivered by flow rate 2.5 μL min^{-1}. Dry gas and drying temperature was set to 5 L min^{-1} and 180 °C. ESI needle voltage was set to 5500 V and nebulization gas pressure was set to 0.2 bar. Spectra were acquired in positive mode in the mass range from 50 to 1600 *m/z* and spectra rate 1 Hz.

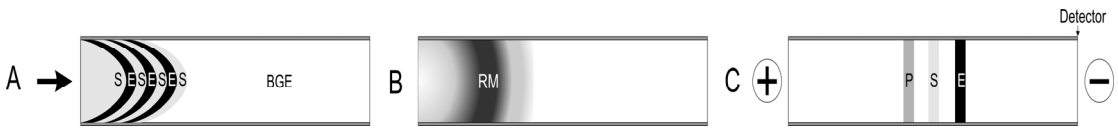

Fig. 1. **Injection procedure.** A – Injected zones. B – Creation of reaction mixture (RM) by diffusion. C – Separation of product (P) substrate (S) and enzyme (E)

3. Results and discussion

3.1. CE-MS method

The method optimization started by selecting appropriate BGE. Ammonium acetate (15, 30 and 50 mM) in pH range 8.5–9.2 was tested. Best results were achieved with 30 mM ammonium acetate, pH 8.7. Selection of nebulization gas pressure was based on stability of total ion electropherograms and peak intensities and best results provided pressure 0.2 bar. ShL study dealt with composition and flow rate. Usage of acidic or alkaline modifier and the nature and percentage of the organic solvent was examined. Acetic acid and ammonia were tested as modifiers. Methanol, acetonitrile and isopropanol were investigated as organic solvent in 1:1 and 1:2 ratios with water. The mixture of isopropanol-water 1:1 (v/v) with 0.5% ammonia showed the highest peak area response. Flow rate was measured in range 1–4 μL min^{-1} and any significant differences between peak areas or intensities were not observed. Therefore flow rate 2.5 μL min^{-1} was used for subsequent experiments.

3.2. On-line incubation

First step of on-line incubation optimization was determination of optimal CYP2C9 concentration in reaction mixture and optimal incubation time. Typical extracted ion electroforeograms are shown on Fig. 2. Repeatability of metabolite production was verified (RSD = 8.9 %; based on peak areas) and external calibration curve was linear in range 25–250 nM. Quantification was based on external calibration. Finally the dependence of reaction rate on substrate concentration was evaluated (Fig. 3). Identification of compounds was performed using standard of metabolite and also using precise mass of parent and fragment ions from MS^2 spectrum (Fig. 4).

4. Conclusions

The new method allowing identification and quantification of enzymatic reaction products within single analysis in on-line CE mode was introduced. Apparent kinetic values obtained with this method (K_m' 4.7 μM and

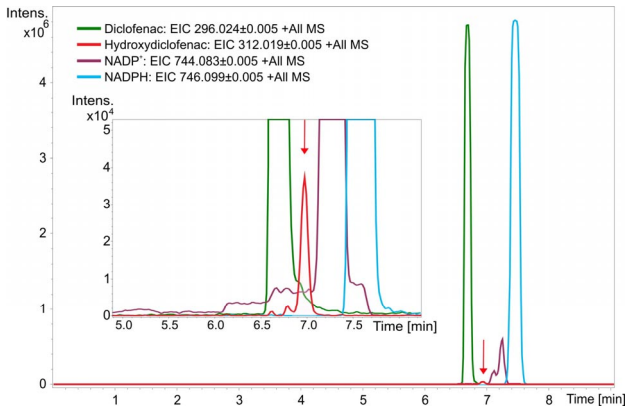

Fig. 2. **Record of analysis after 10 minutes in-capillary incubation of diclofenac**

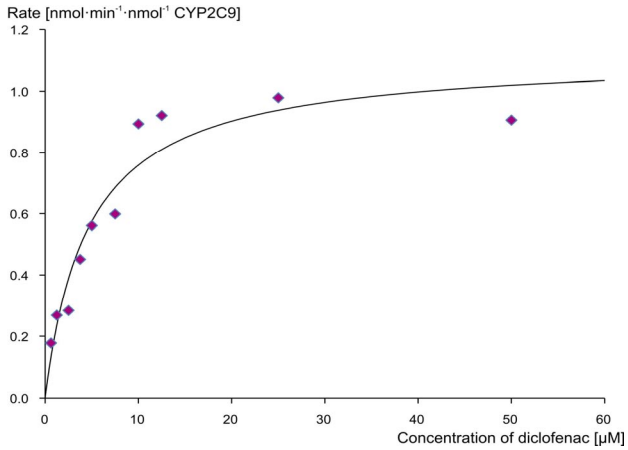

Fig. 3. **Michelis-Menten plot for cytochrome 2C9 reaction with diclofenac**

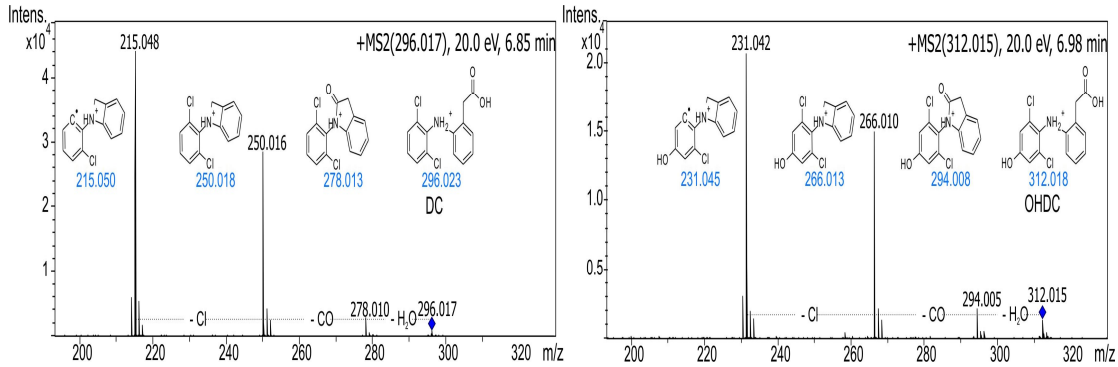

Fig. 4. **MSMS spectrum of diclofenac (DC) and hydroxydiclofenac (OHDC)**

V_{max}' 1.1 nmol min^{-1} $nmol^{-1}$ CYP2C9) were in agreement with previous published data[3]. Principle of reactant's mixing inside capillary based on diffusion and employment of tandem MS detection guarantee generic applicability of method regardless on tested enzyme and substrate.

This study was supported by grant P206/12/G014 financed by Grant Agency of Czech Republic.

REFERENCES

1. Guengerich F. P.: Chem. Res. Toxicol. *21*, 70 (2008).
2. Lin J. H., Lu A. Y. H.: Pharmacol. Rev. *49*, 403 (1997).
3. Řemínek R., Zeisbergerová M., Langmajerová M., Glatz Z.: Electrophoresis *34*, 2705 (2013).

CAPILLARY ISOTACHOPHORESIS OF ANIONS WITH ELECTROSPRAY-IONIZATION MASS-SPECTROMETRIC DETECTION

ZDENA MALÁ, PETR GEBAUER, and PETR BOČEK

Institute of Analytical Chemistry, Academy of Sciences of the Czech Republic, v. v. i., Brno, Czech Republic
mala@iach.cz

Summary

We present ITP-ESI-MS as a powerful tool for selective and sensitive analyses of anionic analytes. Our extended concept of ITP includes besides regular and free-acid ITP also self-maintained ITP in moving boundary systems. Easy theory describes the system properties including their stacking-window diagrams. Simple ESI-compatible electrolyte systems allow flexible tuning with very satisfactory results as demonstrated on the example of analysis of pharmaceuticals in waters.

1. Introduction

The CE-MS combination is a routine technique despite it has lower sensitivity than LC[1]. Replacement of CE by ITP eliminates the dispersion step and analytes remain stacked until they reach the detector and this can enhance the sensitivity by orders of magnitude[2]. Surprisingly the ITP-MS technique was so far applied only scarcely and there are almost no papers about analyses of anions which represent a broad and interesting application field[3]. We present a concept of ITP that allows flexible selection of electrolytes and tuning of their selectivity based on very simple ESI-compatible electrolyte systems, to reach highly sensitive ITP-MS analyses of anions.

2. Experimental

We used a 7100 CE system (Agilent Technologies, Waldbronn, Germany) with a bare fused-silica capillary (100 μm id, 85 cm length) at a running voltage of –20 kV. A commercial CE-ESI-MS interface (Agilent) was used with a coaxial sheath liquid flow (1 % acetic acid + 2 mM ammonium acetate in 50% methanol), supplied via splitter (8 μL min^{-1}). The 6130 single quadrupole mass spectrometer (Agilent) was operated in single ion monitoring negative mode (capillary 3500 V negative; nebulizer pressure 10 psi; drying gas flow 10 L min^{-1}; drying gas temperature 200 °C) for monitoring of $[M-H]^-$ molecules. Nitrogen was supplied by an NM32LA generator (Peak Scientific, Frankfurt, Germany). The CE and MS instruments were controlled and data acquisition performed by ChemStation software (Agilent). Calculations were performed with the freeware program Simul 5 Complex[4].

3. Results and discussion

We use an extended model of ITP[5–7] as shown in Fig. 1 (involving weak acids HA and HB and a weak base R ionizable to RH^+) where both acids HA and HB may be present in both the L and T zones. The system has moving boundary character and behaves as ITP as long as the L-T boundary remains self-sharpening. The condition of stacking of a minor analyte X (acid HX) is

$$u_{\mathrm{ITP,T}} < u_{\mathrm{X,T}} \quad \text{and} \quad u_{\mathrm{X,L}} < u_{\mathrm{ITP,L}} \qquad (1)$$

where $u_{\mathrm{i,j}}$ is its effective mobility in zone j and $u_{\mathrm{ITP,j}} = v_{\mathrm{ITP}}\kappa_{\mathrm{j}}/i$ is the ITP boundary mobility related to zone j (κ_{j} is the specific conductivity of zone j and i is the current density). This condition can be rewritten to the form

$$u_{\mathrm{ITP,T}}\frac{c_{\mathrm{H,T}}+K_{\mathrm{HX}}}{K_{\mathrm{HX}}} < u_{\mathrm{X}} < u_{\mathrm{ITP,L}}\frac{c_{\mathrm{H,L}}+K_{\mathrm{HX}}}{K_{\mathrm{HX}}} \qquad (2)$$

(u_{X} is the ionic mobility of anion X and $c_{\mathrm{H,j}}$ is the H^+ concentration in zone j) that defines the stacking window of the system. Assuming equality we get two curves which plotted in a u_{X} vs. pK_{HX} network demarcate the region of points (u_{X}, pK_{HX}) of analytes X that are stacked in the given ITP system. An example comparing two ESI-compatible ITP systems (composed of formic and propionic acid and ammonium as counterion) is shown in Fig. 2. The points for model analytes diclofenac (Dic), ibuprofen (Ibu) and salicylate (Sal) show different stacking selectivity as only points lying between curves L and T are stacked in the system.

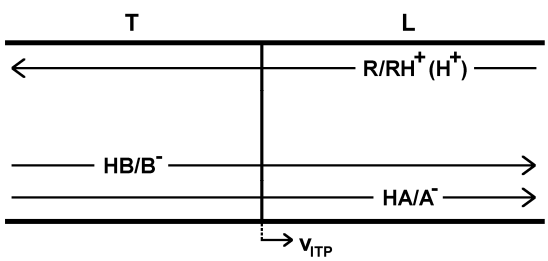

Fig. 1. **Scheme of a moving-boundary ITP system.** L and T are the leading and terminating zones, respectively, and v_{ITP} is the ITP velocity

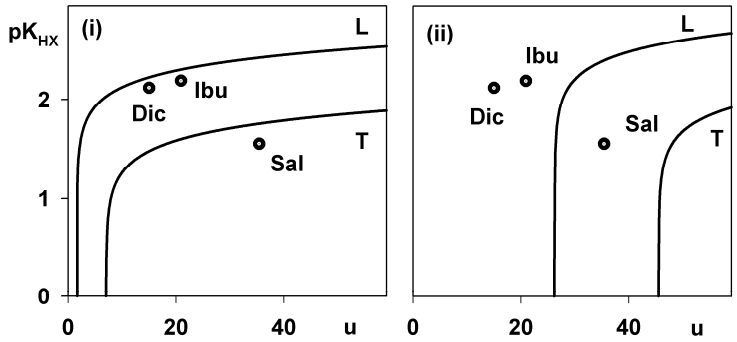

Fig. 2. **Stacking windows of ITP systems.** (i) L: 10 mM formic acid, T: propionic acid; (ii) L: 10 mM formic acid + 8 mM NH_4^+, T: propionic acid (u in 10^{-9} $m^2V^{-1}s^{-1}$)

For simplicity we used the example of regular ITP systems (where HA is missing in zone T and HB is missing in zone L, see Fig. 1) for which the stacking conditions simplify (e.g. condition 1 becomes $u_{B,T} < u_{X,T}$ and $u_{X,L} < u_{A,L}$). Fig. 3a,b show the experimental results of separation of Dic, Ibu and Sal in the systems from Fig. 2. The match well with theory: in system (i) Dic and Ibu are stacked and Sal remains unstacked, in system (ii) the situation is opposite. In Fig. 3c there is the analysis of a real sample (Ibu and Dic in river water) indicating high sensitivity due to ITP stacking in the very simple free-acid system (i) with H^+ as the only counterion.

4. Conclusions

The combination of ITP with ESI-MS allows increasing the sensitivity of electrophoretic analyses by several orders of magnitude. The extended concept of ITP in moving boundary systems brings more flexibility in the selection of electrolyte systems limited by ESI compatibility requirements. Theory allows prediction of the system´s stacking window and easy selectivity tuning. The model allows highly sensitive analyses of anions even in the negative ion mode, e.g. for the analysis of diclofenac and ibuprofen in waters with LOQs on the 10^{-10} M level.

We gratefully acknowledge support by the Grant Agency of the Czech Republic (P206/13/5762) and by Institutional support RVO:68081715 of the Academy of Sciences of the Czech Republic.

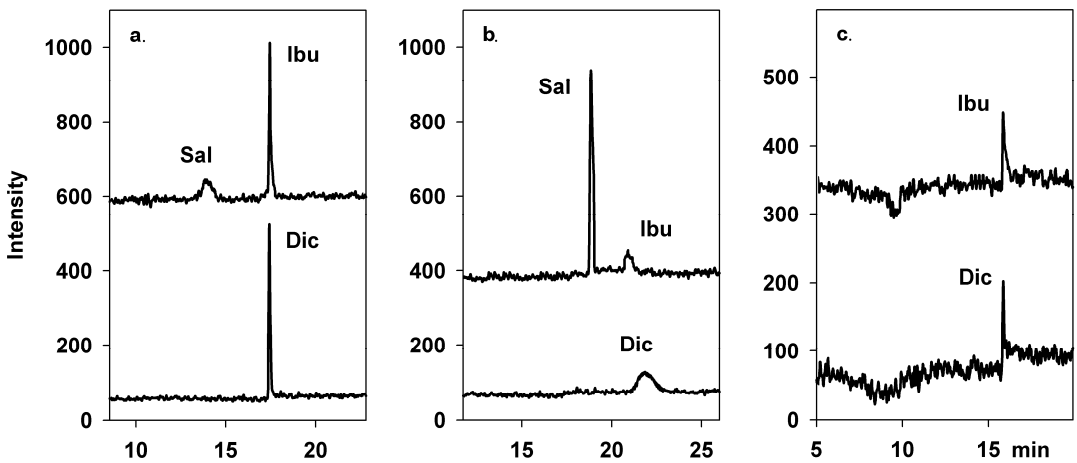

Fig. 3. **Experimental negative single ion monitoring signals for Sal (*m*/*z* 137), Ibu (*m*/*z* 205) (sum in the upper trace) and Dic (*m*/*z* 294, lower trace) of ITP-MS analyses using systems (i) (a,c) and (ii) (b) from Fig. 2.** Sample: (a,b) 10^{-7} M Sal, Ibu and Dic in 2 mM propionic acid, (c) untreated river water (found trace amounts of Dic and Ibuof the order 10^{-10} M). Pressure injection (a,b) 10 mbar for 5 s, (c) 100 mbar for 150 s

REFERENCES

1. Pantůčková P., Gebauer P., Boček P., Křivánková L.: Electrophoresis *30*, 203 (2009).
2. Boček P., Deml M., Gebauer P., Dolník V: *Analytical Isotachophoresis*, VCH Verlagsgesellschaft, Weinheim 1988.
3. Zhao Z. X., Wahl J. H., Udseth H. R., Hofstadler S. A., Fuciarelli A. F., Smith R. D.: Electrophoresis *16*, 389 (1995).
4. Hruška V., Beneš M., Svobodová J., Zusková I., Gaš B.: Electrophoresis *33*, 938 (2012).
5. Malá Z., Pantůčková P., Gebauer P., Boček P.: Electrophoresis *34*, 777 (2013).
6. Malá Z., Gebauer P., Boček P.: Electrophoresis, in press (elps.201300292).
7. Gebauer P., Malá Z., Boček P.: Electrophoresis, in press (elps.201300379).

ADJUSTMENT OF DYNAMIC HIGH RESOLUTION IMAGES OF LIVING CELLS BY COMBINATION OF AN OPTICAL MICROSCOPY IN TRANSMITTING LIGHT, ATOMIC FORCE MICROSCOPY AND IMAGE INFORMATION ANALYSIS

DARIA MALAKHOVA, DALIBOR ŠTYS, and RENATA RYCHTARIKOVA

University of South Bohemia in České Budějovice, FFPW and CENAKVA, Institute of Complex Systems, Nové Hrady, Czech Republic
dmalakhova@frov.jcu.cz

Summary

Presented works is part of the more general project which aims to determine the state of the cell as dynamic self-organizing system. For that, we need to determine position and state of organelles, sub-cellular structures, shape of the cell and events at the cell border. The purpose of current work is to find the solution of the problem of obtaining 3D dynamic images live cell images at maximal resolution and information yield while keeping the cell alive and intact. We combine AFM and optical microscopy in transmitted light. Intermediate results are presented.

1. Introduction

The state of the cell is given by states of its organelles and of the overall organization of the cell. Determination the state of the organelle in the living cell is based on the ability to determine its shape and state. Overall state of the cell is given by its shape, distribution of sub-cellular structures, dynamic processes at cell borders and in its interior.

In order to improve understanding of functioning self organized complex objects we are trying to create the model which help us to get deeper in this problem[1]. For this purpose we are making 3D model of the live cell. This model units in itself combination of image of cell topography with high resolution which have been get by AFM and by in-depth analysis of the stack of images from the optical microscope. The analysis using Rényi information entropy approach[2] enables to eliminate the contribution of the points spread function to the build-up of the image. Theoretical basis of the calculation of the point divergence gain comes from the overall property of the self-organised object, its multifractality. This would solve many basic biological issues, and, in medicinal practice it may serve for identification of abnormalities at different stages of cellular development in artificial fertilization, cancer diagnostics, biocompatibility essays etc.

2. Materials and methods

2.1. Cells cultivation and cells fixation method

For our goals we used cell line MG-63 which bought at Serva cat No.86051601. The cells were grown for the period of the measurement (1–2 days) at 37 °C in a synthetic dropout media with 30% raffinose as the sole carbon source. For AFM scanning cells should be fixed in the petri dish, according to this purpose we fixed cells on the fibronectin using PBS buffer with $Ca^{2+}Mg^{2+}$, Gibco solution and 1 % bovine fetal serum.

2.2. Microscopy

Experiment was done using a versatile sub-microscope – the nanoscope which was developed by the Institute of Complex System FFPW USB in collaboration with Czech fine mechanics and software teams. The optical path are consist of two Luminus 360 light emitted diodes, the condenser system, a firm sample holder and an objective system made of two complementary lenses which allow us to make a change in distance between the objective lens and the sample. The size of the original camera pixel with 40 magnifications was 3434 nm and the size of final pixel after de-mosaicing was 6868 nm. With help of programmable piezo mechanics z-scan was automatically performed and step size was 100 nm.

To identify topography of the cell we have been used atomic force microscope (AFM) NanoWizard 3 produced by JPK Company[3]. Cell scanning was carried in contact mode in liquid. For this type of sample we choose AFM probes MLCT from the Bruker company with resonance frequency 7 kHz and spring constant 0.01 N m^{-1}.

2.3. Point Divergence Gain calculation

The point divergence gain $PDG\alpha,x,y$ is calculated analogously to $PIG_{\alpha,x,y}$ (ref.[4,5]). It is the information increase or decrease achieved by this replacement of the point at position x, y by the point at the same position in the next image $x\ (l + 1)$, $y\ (l + 1)$.

The respective probabilities are pi, the probability of the occurrence of intensity i in the original image l, and pi, $x(l+1)$, $y(l+1)$ the probability of the occurrence of the given intensity in the image where the examined point of coordinates x, y was replaced by the point at the same location in the next image number $l + 1$.

$$PDG_{\alpha,x,y} = \frac{1}{1-\alpha}\, ln\left(\sum_{i=1}^{n} p_i^{\alpha}\right) - \frac{1}{1-\alpha}\, ln\left(\sum_{i=1}^{n} p_{i,x(l+1),y(l+1)}^{\alpha}\right) \quad (1)$$

3. Results and discussion

The comparison of AFM and transmitted light microscopy is complicated by the variance in the points spread function of diffracting object variant in size, shape and interior refractivity index. On the other hand, it has been known for a long time that sub-resolution object may in favorable conditions seen in biological samples[6]. By the method of calculation of the point divergence gain we neglect the point spread function and obtain sharp borders of intracellular objects as they are formed by diffracting elements. In this way we obtain information about the cell at the resolution of one camera pixel, which is in our case 74 nm. Such images may be compared with AFM topographic maps.

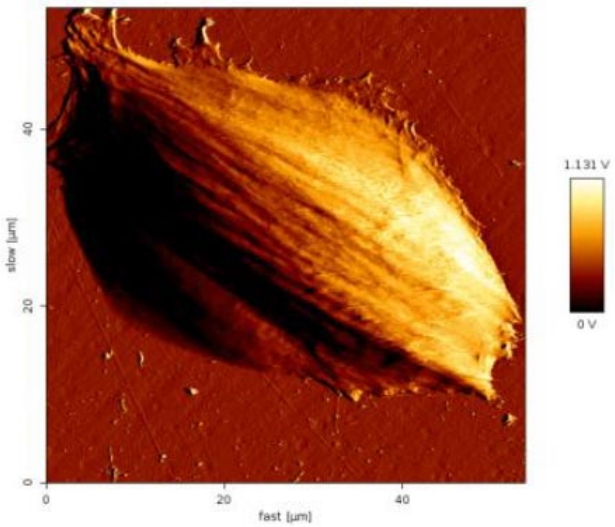

Fig. 1. **AFM image of the living cell MG-63 scanned in contact mode in liquid**

There are a lot of problems occurs during the usage of various AFM set-ups. Fig. 1 shows us one of them. For example it is not clear are we observing cytoskeleton of the cells or it is just some scratches on the cell surface becauce of high force applied during the scanning, or because the cantilever was too stiff for this type of cells.

For comparison of the AFM and optical microscopy information we show the PDG-transformed images from the bright light optical microscope obtained with Rényi coefficient α=4.0 and α=0.5 at the zeroth information change level (Fig. 2). The former enhances shapes of interior objects, the later borders of sub-cellular structures. Theoretical interpretation of these findings is not completed but the technical use is obvious: we identify regions into which the cell is separated (at α=0.5) and identify larger homogeneous object such as organelles (at α=4.0). The former finding has not been reported before, most probably since the information about large-scale unique structures is generally hidden in the dataset until the aspect of general (i.e. non-normal) intensity distribution is implemented in the calculation. The observation at α=4.0 may be to a large extent interpreted in a rather straightforward manner, the level 0 represents objects homogeneously spanning through the two subsequent images, at the level 255 we observe object which either lie only at one level or have mover in the time of positioning of the microscope optics to the next level. However, there are many objects at any intermediate α level which do not have the character of the noise, represent intra-object structures and should be analyzed.

The above mentioned observations, namely the observation of thin objects, is in partial discrepancy with current models of the imaging by the optical microscope. The point spread function spans through the whole space along the optical axis. Thus, the object should be observable at all levels. This we confirm for large object but not in case of smaller and thinner objects. We propose that theory needs to be developed for imaging of

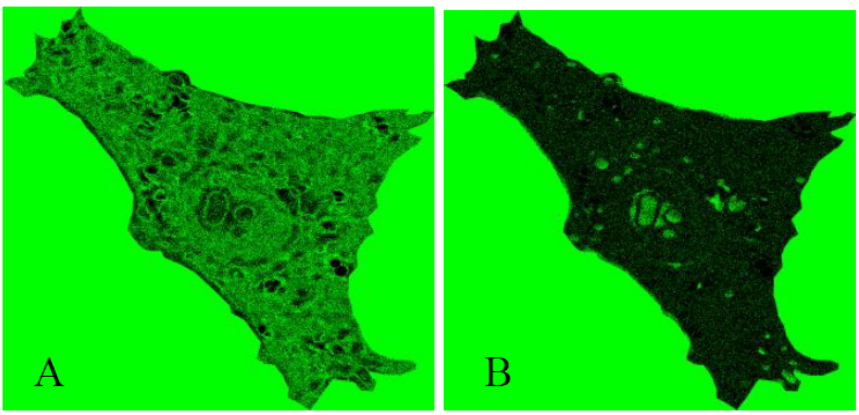

Fig. 2. **Representations of the PDG transformed images at the zeroth level calculated between image 75 and 76 of the cell, with Rényi coefficient at panel A α=0.5 and at panel B α=4.0**

diffracting object, where the diffraction image of the objects is projected on the lens and thus not the image of the point objects gives rise to the interference image, but rays originating from the diffraction image. We do not bring any theoretical solution to the problem, but we believe that is imaginable that along the optical axis, partial re-construction of the original object occurs. And here we bring some evidence, but this needs to be confirmed.

The main aim of the combination of AFM and optical microscopy is calibration of the scale. Any object identified by the transformation of optical microscopy image analysis should lie within the borders of the cell determined by the AFM technology. The report in this article shows technical developments in this direction.

4. Conclusions

In this contribution we present first steps in the avenue towards the complete comparison of the optical microscopy image and AFM topographical image. The final goal is to calibrate the optical image which shall further enable to understand the true state of the living cell without chemical or genetic modification. Moreover, cells are typical example of chemical self-organizing object. The main distinction between cells originating from higher heterotrophic organisms and, for example, the chemical clock, is the existence of "soft" border created by the cell membrane. Thus combination of definition of the border by the AFM and high-resolution dynamic analysis of the state of organelles should only give the answer on origins of cell existence and stability.

This project was supported and co-financed by the GA JU 134/2013/Z and by the CENAKVA CZ.1.05/2.1.00/01.0024.

REFERENCES

1. Zhyrova A., Stys D.: Int. J. Computer Mathematics 2013.
2. Bugrin M.: *Theory of Information: Fundamentality, Diversity and Unification*, World scientific publishing, Singapore 2010.
3. JPK instruments, *NanoWizard Handbook* Version 2.2 02/ 2012.
4. Stys D., Vanek J., Nahlik T., Urban J., Cisar P.: Molecular BioSystems 2011.
5. Stys D., Jizba P., Papacek S., Nahlik T., Cisar P.: *On Measurement of Internal Variables of Complex Self-Organized Systems and Their Relation to Multifractal Spectra*, (Kuipers and Heegaard eds.), Springer, Heidelberg 2012.
6. Stys D., Urban J., Vanek J., Cisar P.: *Analysis of biological time-lapse microscopic experiment from the point of view of the information theory*, Micron 2011.

LIQUID CHROMATOGRAPHY MASS SPECTROMETRY OF SELECTED BENZO-PHENANTHRIDINE ALKALOIDS INCUBATED WITH RAT LIVER MICROSOMES

ADAM MIDLIK[a], KRISTÝNA PĚNČÍKOVÁ[a], IVANA KUŠNYEROVÁ[a], GABRIELA DOVRTĚLOVÁ[b], KRISTÝNA NOSKOVÁ[b], JAN JUŘICA[b], EVA TÁBORSKÁ[a], and ONDŘEJ PEŠ[a]

[a] *Department of Biochemistry, Faculty of Medicine, Masaryk University, Brno,* [b] *Department of Pharmacology, Faculty of Medicine, Masaryk University, Brno, Czech Republic*
379962@mail.muni.cz

1. Introduction

Quaternary benzo[*c*]phenantridine alkaloids (QBAs) belong to a subgroup of isoquinoline alkaloids. They include major sanguinarine (SA) and chelerythrine (CHE) as well as minor QBAs chelirubine (CR), sanguilutine (SL), sanguirubine (SR), chelilutine (CL), and macarpine (MA) (see Fig. 1). The effects of QBAs on biological systems have been studied extensively, especially for commercially available SA and CHE. The results have been summarised in several reviews[1–3]. Limited availability of the minor pentasubstituted QBAs and hexasubstituted MA reduces data concerning their biological effects, yet various anti-proliferative and pro-apoptotic properties have been described[4]. It was shown that although the QBA molecular structures are very similar, the mechanism of their action on the molecular level may be different[5,6]. As pharmacological studies imply that even a small change in the structure may trigger a significant difference in pharmacological activity, it cannot be simply accepted that metabolic routes of all QBAs will be analogous. The metabolic fate of minor QBAs should be intensively studied in order to identify their metabolites, to reveal their toxicity and/or alternate biological effects in different pathways. An approach to reveal the metabolic fate of selected QBAs may employ an *in vitro* model of rat liver microsomes (RLMs) with resulted QBA metabolites to be analyzed by means of liquid chromatography (LC) coupled to hybrid quadrupole time-of-flight (Q-TOF) mass spectrometry (MS).

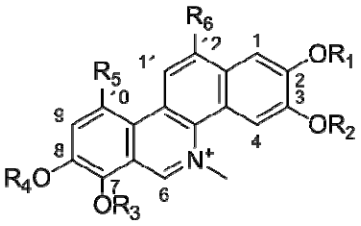

Alkaloid	R_1	R_2	R_3	R_4	R_5	R_6
Sanguinarine (SA)	$-CH_2-$		$-CH_2-$		-H	-H
Chelerythrine (CHE)	$-CH_2-$		$-CH_3$	$-CH_3$	-H	-H
Sanguilutine (SL)	$-CH_3$	$-CH_2$	$-CH_3$	$-CH_3$	$-OCH_3$	-H
Chellilutine (CL)	$-CH_2-$		$-CH_3$	$-CH_3$	$-OCH_3$	-H
Sanguirubine (SR)	$-CH_3$	$-CH_3$	$-CH_2-$		$-OCH_3$	-H
Chelirubine (CR)	$-CH_2-$		$-CH_2-$		$-OCH_3$	-H
Macarpine (MA)	$-CH_2-$		$-CH_2-$		$-OCH_3$	$-OCH_3$

Fig. 1. **Benzo[*c*]phenanthridine alkaloid structures**

2. Experimental

2.1. Extraction and isolation of QBAs

SA, CHE, CL, and CR were isolated according to a method described by Slavik et al.[7]. Isolation and purification step was performed by means of semi-preparative reversed-phase (RP) chromatography. The purity of alkaloids was > 90 %.

2.2. Isolation of RLMs

Research male rats (Wistar albino) of the same age and weight were killed by decapitation and subjected to laparotomy. A liver sample (4 g) was homogenized, centrifuged and the total protein was determined by the Lowry method and bovine serum albumin as standard.[8] Aliquots were stored in –80 °C until needed.

2.3. Incubation, extraction and analysis of samples

Each alkaloid (50 μL) was vortexed with 50 μL of RLMs in a buffered (50 mM phosphate, pH 7.4) NADPH generating system (glucose-6P dehydrogenase, glucose-6P) for 30 min. The reaction was stopped by addition of 100 μL of methanol and transferring to an ice bath.

Metabolites were purified by adding 1 mL of MeOH:ACN:formic acid (50:50:0.02) into a 100 μL aliquot of the incubation mixture, followed by vortex and centrifugation. A small portion of the supernatant was five times diluted and injected (20 μL) onto an LC column.

2.4. LC MS

LC MS method was established using Dionex Ultimate 3000RS (Thermo Scientific, Sunnyvale, CA) module. Compound separation was achieved with a 3.0 × 150 mm, 4 μm Synergi RP-Max C18 column at 23 °C and a flow rate of 0.5 mL min^{-1}. A binary mobile phase system

consisted of 0.1% formic acid (A) and LC-MS grade ACN (B). Mobile phase B was increased from 20 % to 40 % for 10 min and then to 80 % for next 10 min. It was kept constant for 10 min followed by equilibration to the initial conditions for 3.0 min. A total HPLC run was 33 min. The HPLC system was connected to a MicrOTOF-QII (Bruker, Germany) mass spectrometer, operated in positive electrospray ionization mode. The ionization conditions were set by the software as the following: Capillary voltage 4500 kV, end plate offset –0.5 kV, source temperature 220 °C, desolvation gas (nitrogen) flow 10 L min^{-1}, nebulizer (nitrogen) pressure 3 bar, collision cell voltage 35 eV.

3. Results and discussion

LC MS and MS/MS spectra were first investigated to obtain the elemental formula of each compound. Identification of target compounds then relied on isotope pattern matching and combination of MS/MS and retention behavior. Products of incubation for each QBA are summarized in Table I. QBAs were found to undergo reduction to dihydro-derivatives (+2 Da) and/or demethylation (–14 Da) of both parent and reduced compounds. *O*-demethylation was proposed since retention times of *N*-demethylated products would have considerably increased due to the loss of the quaternary nitrogen. Identity of reduced compounds was verified by the reaction of the original incubation mixture with an excess of $NaBH_4$, resulting in the pure alkaloid and the *O*-demethylated product to be further reduced to its respective dihydro (DH) compound.

4. Conclusions

Selected QBAs were, when incubated with RLMs, found to provide dihydro-derivatives with CHE, CL, and CR correspondingly metabolizing to mono *O*-demethylated products. Absence of additional metabolites (hydroxylation, ring-opening reactions) might be explained by low activity of cytochrome P450 isoenzymes and/or insufficient time of incubation.

The work was supported by Czech Ministry of Education, Youth and Sports (LH12176-KONTAKT II) and Science Foundation of Masaryk University (MUNI/ A/0818/2012).

REFERENCES

1. V. Simanek, R. Vespalec, A. Sedo, J. Ulrichova, J. Vicar, in *Chemical Probes in Biology: Science at the Interface of Chemistry, Biology and Medicine*, ed. by M. P. Schneider, 2003, Vol. 129, pp. 245-254.
2. Z. Dvorak, V. Kuban, B. Klejdus, J. Hlavac, J. Vicar, J. Ulrichova, V. Simanek: Heterocycles *68*, 2403 (2006).
3. A. Zdarilova, J. Malikova, Z. Dvorak, J. Ulrichova, V. Simanek: Chem. Listy *100*, 30 (2006).
4. I. Slaninova, K. Pencikova, J. Urbanova, J. Slanina, E. Taborska: Phytochem. Rev. DOI 10.1007/s11101-013 -9290-8 (2013).
5. W. C. Tang, I. Hemm, B. Bertram: Planta Med. *69*, 97 (2003).
6. M. L. Colombo, E. Bosisio: Pharm. Research *33*, 127 (1996).
7. J. Dostal, J. Slavik: Chem. Listy *94*, 15 (2000).
8. O. H. Lowry et al.: J. Biol. Chem. *193*, 265 (1951).

Table I
The retention time, exact mass and elemental composition of selected QBAs after 30 min incubation with RLMs

Alkaloid	Detected products	t_r (min)	Ion	Observed m/z	Calculated m/z	error (ppm)	Sum formula [M]
SA		4.4	$[M]^+$	332.0927	332.0923	-1.3	$C_{20}H_{14}NO_4$
	DHSA	22.1	$[M+H]^+$	334.1069	334.1079	3.1	$C_{20}H_{15}NO_4$
CHE		5.7	$[M]^+$	348.1241	348.1236	-1.5	$C_{21}H_{18}NO_4$
	DHCHE	21.5	$[M+H]^+$	350.1391	350.1392	0.4	$C_{21}H_{19}NO_4$
	O-demethylated CHE	4.4	$[M]^+$	334.1071	334.1079	2.5	$C_{20}H_{16}NO_4$
	O-demethylated DHCHE	17.5	$[M+H]^+$	336.1235	336.1236	0.2	$C_{20}H_{17}NO_4$
CL		7.1	$[M]^+$	378.1351	378.1341	-2.5	$C_{22}H_{20}NO_5$
	DHCL	21.1	$[M+H]^+$	380.1483	380.1498	3.9	$C_{22}H_{21}NO_5$
	O-demethylated CL	5.7	$[M]^+$	364.1180	364.1185	1.4	$C_{21}H_{18}NO_5$
	O-demethylated DHCL	16.2	$[M+H]^+$	366.1331	366.1341	2.9	$C_{21}H_{19}NO_5$
CR		6.1	$[M]^+$	362.1033	362.1028	-1.2	$C_{21}H_{16}NO_5$
	DHCR	21.9	$[M+H]^+$	364.1168	364.1185	4.7	$C_{21}H_{17}NO_5$
	O-demethylated CR	4.7	$[M]^+$	348.0865	348.0872	2.0	$C_{20}H_{14}NO_5$
	O-demethylated DHCR	17.8	$[M+H]^+$	350.1027	350.1028	0.4	$C_{20}H_{15}NO_5$

USING DIFFERENT ELECTROPHORETIC METHOD FOR THE DETERMINATION OF THE AFFINITY CONSTANTS OF SALICYLIC ACID AND BSA

LENKA MICHALCOVÁ and ZDENĚK GLATZ

Department of Biochemistry, Faculty of Science and CEITEC – Central European Institute of Technology, Masaryk University, Brno, Czech Republic lenna@mail.muni.cz

Summary

The capillary electrophoresis fontal analysis (CE-FA), Hummel Dreyer methods (HD) and affinity capillary electrophoresis (ACE) were used to study the affinities between salicylic acid (SA) and bovine serum albumin (BSA). The binding constant (Ka) was measured by all these methods. The Ka values obtained from CE-FA (5.66 ± 0.22 × $10^3 M^{-1}$), HD methods with internal (2.83 ± 0.23 × $10^3 M^{-1}$) and external (2.28 ± 0.12 × $10^3 M^{-1}$) calibration are in agreement. The comparison of results and other conditions shows the best measurement methods are CE-FA and HD with external calibration.

1. Introduction

The binding constant (Ka) is commonly used to describe the strength of binding between ligand such as drug and protein. The strength of the interaction has a significant effect on the biological activity of the drug, and knowledge of the nature and extent of drug-protein binding can help us to understand the pharmacokinetics and pharmacodynamics of a drug[1]. The advantage of capillary electrophoresis (CE) is very low sample consumption and a high resolution. It does not require the highly purified samples, immobilization or labelling of any of the interacting species. The investigated interaction takes place in a solution, which can be simulated physiological conditions[2].

The main objectives of this study were to determine the Ka of the model system (BSA – SA) using several CE based methods, compare their results and their requirements – time preparation, time analysis, simplicity of evaluation and repeatability of measurements.

2. Experimental

The uncoated fused silica capillary was 58.5/50 cm (L_{tot}/L_{eff}) with I.D. of 75 μm. Operational voltage of 24 kV was performed in normal polarity and the detection wavelength was set to 214 nm. The temperature of the capillary was maintained at 25 °C. The other conditions of optimized methods are summed in Tab. I.

3. Results and discussion

In order to establish the Ka, three CE based methods – CE-FA, HD, ACE were chosen. Representative electropherograms of the CE-FA method for complex BSA - SA and a standard solution of SA are shown in Fig. 1. CE-FA provides good repeatability and good fitting of data points (Tab. II).

HD was carried out in two forms – with internal or external calibration. Representative electropherograms of the HD method are shown in Fig. 2.

The peak area and peak height were tested for evaluation of binding curve. The peak area was found a better parameter than the peak height. The internal and external calibrations were tested as well, and it is the external calibration that provides better repeatability and lesser scatter of data points (Tab. II).

Table I
Summary of capillary electrophoresis conditions

	CE-FA	HD	ACE
Background electrolyte (BGE)	borate buffer (15mM borax was adjusted to pH 8.5 with 60mM boric acid)		
	neat BGE without additives	with different amounts (0 – 800 μM) of SA	with different amounts (0 – 20 μM) of BSA
Sample	50 μM BSA + 10 -1000 μM SA	50 μM BSA	1 mM SA + 0.05% DMSO
Capillary treatment	Pre-analysis: 2 min 1 M HCl 1 min water 5 min 0.1 M NaOH 1 min water 2 min BGE 3 min 24 kV BGE Post-analysis: 1 min water		Pre-analysis: 3 min 1 M NaOH 2 min water 3 min BGE Post-analysis: 1 min water

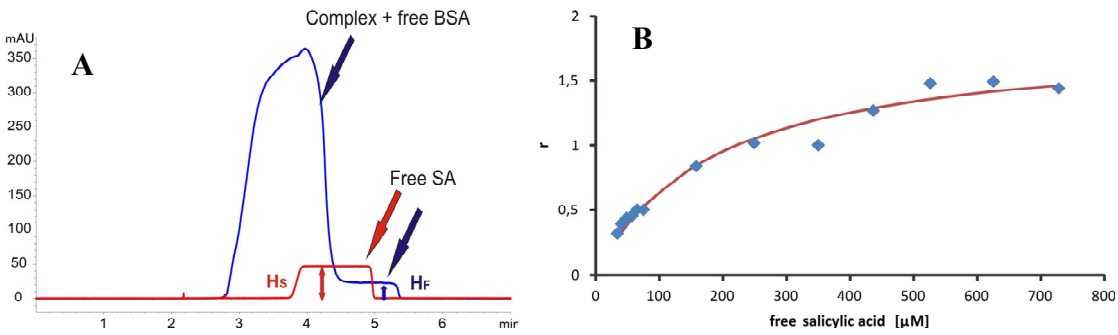

Fig. 1. **Set of representative results obtained with the CE-FA method.** A) Electrophoreograms o free SA for calibration curve and complex BSA – SA. B) Typical binding curve obtained for BSA – SA with CE-FA

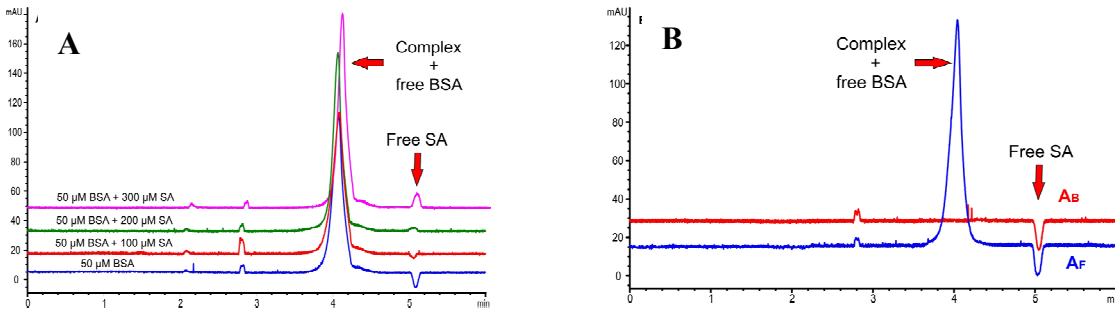

Fig. 2. **Typical results of HD methods. Both examples are measured in BGE with 200 µM SA.** A) Internal calibration. B) External calibration

Table II
Summary of results

	Ka · 10^3 l/mol	n
CE-FA	5.66 ± 0.22	1.8 ± 0.2
HD area internal calibration	2.83 ± 0.23	2.6 ± 0.5
HD area external calibration	2.28 ± 0.12	1.7 ± 0.3

The comparison of data points obtained with different HD modification is shown in Fig. 3. The binding curve obtained with the CE-FA is included as a reference.

The last tested method was ACE. Representative electropherograms of ACE are shown in Fig. 4. The advantage of the method is that it does not require a calibration for measurement of binding constant. The several types of flushing procedure were tested for better repeatability of analysis. The procedure with the smallest RSD for a run to run analysis was chosen as the best washing procedure. However, the repeatability between day to day analyses was insufficient.

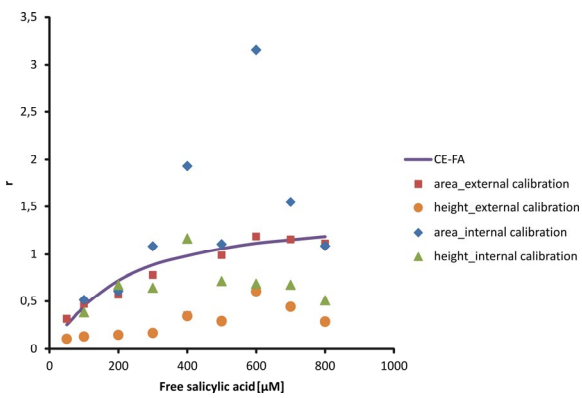

Fig. 3. **Binding curves of BSA – SA obtained by HD methods**

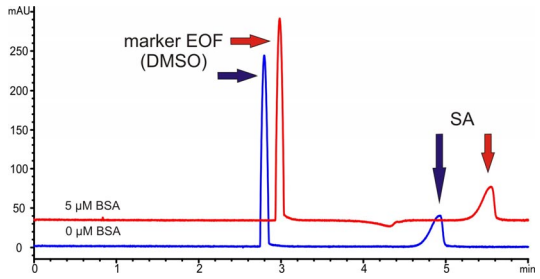

Fig. 4. **Typical electropherograms of ACE**

4. Conclusions

The Ka was measured by several capillary electrophoretic methods. Their comparison shows that the simplest methods (according to amount of different BGEs and different samples) are CE-FA and HD with external calibration. But CE-FA data points contain a lesser scatter than HD data points do. The HD method with internal calibration requires more demanding preparation of sample.

This work was supported by grant P206/12/G014 from the Czech Science Foundation.

REFERENCES

1. Sharma R., Choudhary S., Kishore N.: Eur. J. Pharm. Sci. *46*, 435 (2012).
2. Vuignier K., Schappler J., Veuthey J. L., Carrupt P. A., Martel S.: Anal. Bioanal. Chem. *398*, 53 (2010).

ELECTROPHORETIC MOBILITY MEASUREMENTS OF A MULTIVALENT RED DYE SPADNS

PAVLA PANTŮČKOVÁ, PAVEL KUBÁŇ, and PETR BOČEK

Institute of Analytical Chemistry of the Academy of Sciences of the Czech Republic, v. v. i., Veveří 97, CZ-602 00 Brno, Czech Republic
pantuckova@iach.cz

Summary

Measurements of the electrophoretic mobility of an anionic dye 4,5-dihydroxy-3-(*p*-sulfophenylazo)-2,7-naphthalene disulfonic acid trisodium salt (SPADNS), which is a commonly used anionic dye, are described in this contribution. Electrophoretic mobilities of SPADNS were measured in various buffer solutions covering the pH range of 2.4–9.1. Effective electrophoretic mobilities of SPADNS measured in these buffers varied between 50.5 × 10^{-9} m^2/Vs and 60.5 × 10^{-9} m^2/Vs with an average effective mobility of 55.0 × 10^{-9} m^2/Vs.

1. Introduction

The determination of electrophoretic mobilities of multivalent dyes and determination of their p*K*s is very often neglected in the literature. These measurements are not trivial and usually result into data, which are not easy to interpret and are therefore often not published. Electrophoretic mobility of SPADNS was not published so far. However, SPADNS is often used as an attractive visible compound for measurement of e. g. precise timing for time switching between isotachophoretic and capillary electrophoretic step[1]. The need for the determination of its electrophoretic mobility started to be important in our actual research concerning micro-electromembrane extractions using electrically induced transfer of charged analytes across free liquid membranes[2], since SPADNS is well suitable for observation of the transfer of analytes and it offers intensive colour even at low concentrations. Chemical structure of SPADNS is depicted in Fig. 1.

2. Experimental

Effective mobilities of SPADNS were measured in 5 different buffer solutions within the pH range of 2.4–9.1: 1 M acetic acid (HAc), pH 2.4; 10 mM Histidine (His) + 50 mM HAc, pH 4.1; 20 mM 2-Morpholinoethanesulfonic acid monohydrate (MES) + 20 mM His, pH 6.1; 20 mM Tris-hydroxymethylaminomethane (Tris) + 10 mM HCl, pH 8.1; 50 mM Tris + 5 mM HCl, pH 9.1. Electrophoretic separations were performed in a fused silica capillary of 31.5/24.5 cm total/effective length, 75 µm id/365 µm od, applied voltage of = 8/–8 kV and injection for 3 s at 3 mbar corresponding to the injected sample length of 4 mm. Commercial capillary electrophoresis apparatus, Agilent 7100, was used for the experiments. The calculations of electrophoretic mobilities were done according to ref.[4].

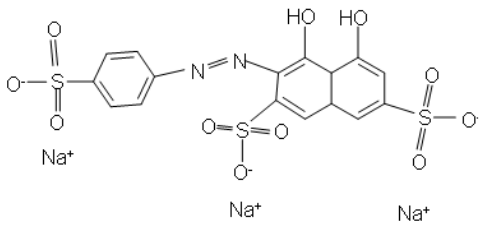

Fig. 1. **The chemical structure of SPADNS** (pK -3.0, -2.0, 3.55 , ref.[3]).

3. Results and discussion

The mobilities of the electroosmotic flow (μ_{EO}) were measured at positive polarity using mesityl oxide as an analyte, which was detected at 254 nm, see Table I. The results of the effective mobilities of SPADNS, which were measured at negative polarity, are summarized in Table I as well. For the measurements of SPADNS mobilities, the apparatus was set at the maximum of its absorbance at 490 nm.

4. Conclusions

Measurements of electrophoretic mobility of SPADNS were performed in various buffer solutions. Mobility of electroosmosis increased with the pH of buffer solutions according to the theory and reached maximum value at pH 9.1 as expected. On the other hand effective electrophoretic mobilities of SPADNS showed no pH dependence within pH range of 2.4–9.1. It means that true p*K* values of SPADNS can be expected below 2. The relative large variation range confirms the empirical experience that mobilities of multivalent dyes are not easy to be measured. A possible explanation may be the sorption effects of the dye ions to capillary wall due to the presence of a lot of polar functional (azo- and hydroxyl) groups. Measurements of effective mobilities of

Table I
Comparison of μ_{EO} and μ_{eff} (SPADNS) in selected buffer solutions

pH	μ_{EO} [$\times 10^{-9}$ m^2/Vs]	μ_{eff}(SPADNS) [$\times 10^{-9}$ m^2/Vs]
2.4	14.6	54.8
4.1	17.2	60.5
6.1	25.1	56.0
8.1	30.4	50.5
9.1	47.5	53.4

The effective mobility of SPADNS varied within the range of 50.5–60.5 × 10^{-9} m^2/Vs. The average effective mobility corresponds to 55.0 × 10^{-9} m^2/Vs.

multivalent dyes are therefore feasible, note however, that these might be dependent on buffer solution composition and pH value.

Financial support from the Academy of Sciences of the Czech Republic (Institute Research Funding RVO: 68081715) and the Grant Agency of the Czech Republic (Grant No. 13-5762S) is gratefully acknowledged.

REFERENCES

1. Pantůčková P., Křivánková L.: Electrophoresis *31*, 3391 (2010).
2. Kubáň P., Boček P.: Submitted for publication.
3. Hirokawa T., Omori A., Yokota Y., Hu J.-Y., Kiso Y.: J. Chromatogr. *585*, 297 (1991).
4. Foret F., Křivánková L., Boček P.: *Capillary Zone Electrophoresis,* pp. 7–19, VCH Weinheim 1993.

POLYDOPAMINE COATED CAPILLARIES FOR CE SEPARATIONS

JAN PARTYKA[a,b], FRANTISEK FORET[a], THI THU VU[c,d], and JAN SUDOR[c,d]

[a] *Institute of Analytical Chemistry of the AS CR, v.v.i., Brno, Czech Republic,* [b] *Department of Chemistry, Faculty of Science, Masaryk University, Brno, Czech Republic,* [c] *Université de Toulouse; UPS; UMR 152 Pharma-Dev; Université Toulouse 3, Faculté des Sciences Pharmaceutiques, F-31062 Toulouse cedex 09, France,* [d] *Institut de Recherche pour le Développement (IRD); UMR 152 Pharma-Dev; F-31062 Toulouse cedex 09, France*
partyka@iach.cz

Summary

We have tested CE separation of selected samples in capillaries with polydopamine modified surface. The capillaries were modified by polydopamine or polydopamine with an additive. The polydopamine coating with additive represents a simple and effective procedure for capillary alteration by another modificator such as hydroxyethyl cellulose, hydroxypropyl cellulose etc. In this work, we represent separation data from PrinCE system with UV detection for peptides, proteins and oligosaccharides labeled by 2-aminobenzoic acid.

1. Introduction

Commonly used techniques for modification of capillaries require chemicals with a reactive group which allows a binding to capillary wall. Application of these compounds is often problematic because of their reactivity and modification process usually requires some specific conditions such as high temperature or nonaqueous solvent. The represent surface modification was inspired by mussels which polymerize dopamine in water solution to form adhesive[1].

2. Experimental

The capillaries were modified by dopamine in TRIS/HCl (50 mM, pH 9.0). Ammonium persulfate was added to the dopamine solution to obtain faster polymerization and more uniform surface coatings. We experimented with several additives because of improvement separation properties of capillaries. These additives were added into the dopamine solution before polymerization.

The separations were measured using PrinCE autosampler with UV detection (214 nm). The peptides and proteins were used without any another labeling. A dextran ladder was used as sample of oligosaccharides. Because of absence any chromophore in molecules of oligosaccharides, labeling by 2-aminobenzoic acid was necessary. The all separations were performed in 6-aminocaproic acid/acetic acid (20 mM, pH 4.8) as a background electrolyte[2].

3. Results and discussion

In parallel with the capillaries, we have also modified flat surfaces and characterized them with water contact angle (WCA) measurements, atomic force microscopy (AFM) in a tapping mode, cyclic voltammetry (CV) and by the measurements of the endoosmotic flow. The WCA measurements clearly showed that all studied surfaces (Si, SiO_2, Au, Cu, SU8 and PDMS) were covered with the DOPA film (WCA for the DOPA film was between 50.5–53.9° for all the surfaces). The AFM studies showed an improved uniformity of the DOPA coatings when ammonium persulfate was utilized in the polymerization mixture. The thickness of the deposited films was also measured by AFM and was found to be close to 10 nm after 3 hrs of film deposition. However, we can increase the film thickness by repeating the coating procedure with fresh solutions. The DOPA films were also studied by cyclic voltammetry and it was observed that the oxidation/reduction peaks of an electroactive probe (ferrocyanide) disappeared after a gold surface was treated with DOPA solution.

We have compared separations in bare fuse silica capillary, capillary coated by polydopamine and capillaries coated by polydopamine with additive. Hydroxyethyl cellulose (HEC) from 90 to 1300 kDa, hydroxypropyl cellulose (HPC) from 100 to 1000 kDa and polyvinyl alcohol (PVA) 70 kDa were tested as the additive. Measurement of endoosmotic flow by dimethoxysulfoxide showed prolongation of migration times in polydopamine-coated capillary and in polydopamine-coated capillaries with additive. The endoosmotic flow was suppressed in capillaries coated by polydopamine with additive more than only polydopamine and the migration times were various in dependence on kind of additive, e.g. when HEC (90 kDa) was used, no EOF was observed.

A mixture of seven peptides was used as a model for testing of capillaries. The separation was the fastest thanks to the strongest EOF and at the same time the worse in bare fuse silica capillary. Effective separations were accomplished by coated capillaries. A resolution of each

peak was sufficient but only migration times were various.

Unfortunately, separations of proteins were not successful. We tested a mixture of four proteins, but no clear peaks were observed. These problems were partially suppressed when we used stacking effect because of peaks self-focusing.

The best separations results of 2-aminobenzoic labeled oligosaccharides were accomplished by polydopamine coated capillary and by polydopamine with HPC 100 kDa coated capillary. The separations had better resolution than separation in the bare fuse silica capillary. A small disadvantage can be prolongation of migration times of oligosaccharides but it can be overcome by using higher separation voltage.

4. Conclusions

In this work, we presented a new possibility of capillary coating. The polydopamine coating appears as promising procedure because of simple reaction conditions in water solution. Moreover, it is possible to use polydopamine as resin during grafting of HEC, HPC etc. The capillaries with these coatings are suitable for CE separation of small molecules such as peptides or oligosaccharides.

This work was supported by the Grant Agency of the Czech Republic (P301/11/2055), the Academy of Sciences of the Czech Republic (M200311201) and the institutional research plan (RVO: 68081715). This project is co-financed by the European Social Fund and the state budget of the Czech Republic (CZ.1.07/2.3.00/20.0182). Thi Thu Vu benefitted from the fellowship of the University of Hanoi.

REFERENCES

1. Lee H., Dellatore S. M., Miller W. M., Messersmith P. B.: Science *318*, 426 (2007).
2. Foret F., Szökő E., Karger B. L.: Electrophoresis *14*, 417 (1993).

ISOQUINOLINE ALKALOIDS OF THE CZECH AND CHINESE CULTURE OF *MACLEAYA MICROCARPA* (MAXIM.) FEDDE

KRISTÝNA PĚNČÍKOVÁ[a], ONDŘEJ PEŠ[a], PETR TÁBORSKÝ[b], ZHI-HONG JIANG[c], and EVA TÁBORSKÁ[a]

[a] Department of Biochemistry, Faculty of Medicine, Masaryk University, Brno, Czech Republic, [b] Department of Chemistry, Faculty of Science, Masaryk University, Brno, Czech Republic, [c] State Key Laboratory of Quality of Chinese Medicine Research, Macau University of Science and Technology, AvenidaWai Long, Macao, PLR
k.pencikova@mail.muni.cz

1. Introduction

Macleaya microcarpa (Maxim.) Fedde belongs, together with *M. cordata* (Willd.) R. Br. and their interspecific hybrid *Macleaya x kewensis* Turill, to the genus *Macleaya*, family Papaveraceae. Quaternary benzophenanthridine alkaloids (QBAs) sanguinarine (SA), chelerythrine (CHE), chelirubine (CR), chelilutine (CL) and the rarely occurring macarpine (MA) are the most interesting bioactive substances. While the major benzophenanthridine alkaloids SA and CHE are available commercially and have been the subjects of numerous biological studies, minor QBAs remained unnoticed for a long time due to their limited availability. Not long ago, first biological studies[1–3] described the effects of these alkaloids on cells and identified a number of interesting properties, which puts these alkaloids in the center of interest for further research. Minor QBAs display strong anti-proliferative and apoptotic activity *in vitro*[2]. MA has been reported as promising fluorescent probe for cell nuclei labeling and visualization of various stages of the cell cycle in fluorescence microscopy and flow cytometry[1]. In addition, polycyclic, planar structure of the quaternary form allows intercalation of these alkaloids into DNA[4].

Hence, the essential assumption for further studies of minor QBAs is the necessity to obtain these alkaloids in sufficient quantities. As they are not available commercially and synthesis is rather unsatisfactory[5], isolation from the plant material seems to be the best approach for their production.

M. microcarpa is a perennial herb whose origin is in central China. In conditions of middle Europe, *Macleaya* is successfully grown and reproduced vegetatively. The aim of this presentation is to compare the content of alkaloids in the Czech and Chinese culture.

2. Experimental

M. microcarpa was grown in The Centre of Medicinal Plants of Masaryk University in Brno. One-year-old culture was harvested in September 2009, fourteen years old culture was harvested in July 2010. Chinese *M. microcarpa* was collected in mountains in province Shan'xi in June 2012. It was not possible to determine the age of this culture.

The plant material was wiped, dried, finely grounded and extracted by methanol in FexIKA apparatus (IKA, Germany), which is based on the fluidized bed extraction. The extraction time was 16×15 min. After extraction, the individual extracts were evaporated to 25 mL.

Subsequently, the extracts were diluted 1:1 with HPLC mobile phase and filtered through a 0.45 μm syringe filter. Samples were analyzed by reversed phase HPLC with UV detection. Moreover, identification of alkaloids was confirmed by HPLC-MS/MS.

The HPLC analyses were performed using an HPLC apparatus consisting of a high pressuregradient pump LC-20AD, DAD detector SPD M20A (Shimadzu, Japan), ECOM syringe loading sample injector (ECOM, Czech Republic) with external sample loop 20 μl and C-12 column Synergi Max-RP 80A (4 μ, 150×4.60 mm ID) (Phenomenex, USA). The extract analyses were performed using gradient elution. The mobile phase was prepared from a stock solution containing sodiumheptanesulfonate (0.01 mol L^{-1}) and triethylamine (0.1 mol L^{-1}) in redistilled water, pH 2.5 was adjusted by phosphoric acid. The solution A and B contained 25 % and 60 % (v/v) of acetonitrile, respectivelly. The following elution profile was employed: 0–1 min isocratically 20 % B; 10 min 50 % B; 20 min 100 % B; 20–30 min isocratically 100 % B. The flow rate was set to 0.5 mL min^{-1} and the detection was performed by the DAD detector at 280 nm.

3. Results and discussion

One of the first comprehensive studies of *M. microcarpa* came from Slavík[6]. For a long time, *M. microcarpa* remained unnoticed, while *M. cordata* has been studied and cited as a source of benzophenanthridines SA and CHE. A detailed study of *M. microcarpa* has been published recently; it includes changes in alkaloid content during the entire vegetation period[7].

The results of current analysis showed that allocryptopine (ALL) is the main alkaloid of the underground part from both cultures. Other major alkaloids include protopine (PRO) and CHE (Tab. I), small amounts of berberine and coptisine were detected as well.

Table I
The alkaloid content in the Czech and Chinese culture of *Macleaya microcarpa*. The experiments were performed in a duplicate. The amount of alkaloids is expressed as mass of alkaloid (mg) per a gram of the dry drug ± standard deviation

Age of the plant (years)	PRO	ALL	SA	BER	CHE	CR	CL	MA
	mg/g ± SD	mg/g ± SD	mg/g ± SD	mg/g ± SD	mg/g ± SD	mg/g ± SD	mg/g ± SD	mg/g ± SD
1 (Czech)	13.659±2.089	50.870±9.166	1.886±0.322	0.063±0.015	2.704±0.428	0.826±0.117	0.232±0.046	0.237±0.075
14 (Czech)	10.723±1.360	56.498±4.114	4.713±0.463	0.093±0,012	11.267±2.264	3.242±0.545	1.317±0,254	1.907±0.385
? (Chinese)	3.573±0.456	22.679±3.514	1.832±0.286	0.201±0,028	2.998±0.543	1.864±0.335	0.995±0.182	0.948±0.260

In addition, presence of *N*-methylcanadine was confirmed by HPLC-MS/MS in the Chinese culture and in the one-year-old Czech culture. In the older Czech culture, this alkaloid was not detected at all.

The same minor QBAs - CR, CL and MA were found in both cultures, though their amounts were significantly higher in the older Czech culture (approximately 4-fold for CR, 6-fold for CL and at least 8-fold for MA, see Tab. I). Nevertheless, this culture is 14 years old, which is not perspective for routine harvest and alkaloid isolation.

Despite the unknown age of the Chinese culture of *M. microcarpa*, CR, CL and MA amounts were approximately only 2-fold lower than in older plants encouraging the option to harvest *M. microcarpa* in its natural habitat.

4. Conclusion

Currently, the main source of QBAs is isolation from plant material.Therefore, it is necessary to constantly search for new possibilities and cultures, which are able to accumulate these alkaloids in sufficient quantities.

The financial support of this work by The Ministry of Education of Czech Republic (project KONTAKT II LH12176) and by the Masaryk University Project of Specific Research (SVMUNI/A/0818/2012) is gratefully acknowledged.

REFERENCES

1. Slaninová I., Slanina J., Táborská E.: Cytometry A *71*, 700 (2007).
2. Slaninová I., Slunská Z., Šinkora J., Vlková M., Táborská E.: Pharm. Biol. *45*, 131 (2007).
3. Slunská Z., Gelnarová E., Hammerová J., Táborská E., Slaninová I.: Toxicol. In Vitro *24*, 697 (2010).
4. Hossain M., Kumar G. S.: J. Thermodyn. *41*, 764 (2009).
5. Ishikawa T., Saito T., Ishii H.: Tetrahedron *51*, 8447 (1995).
6. Slavík J., Slavíková E.: Chem. Listy *48*, 106 (1954).
7. Pěnčíková K., Urbanová J., Musil P., Táborská E., Gregorová J.: Molecules *16*, 3391 (2011).

PREPARATION OF LOW-COST MICROFLUIDIC DEVICES USING AN OFFICE LAMINATOR

LENKA VOJTKOVÁ, PAVLÍNA SVOBODOVÁ, ANDREA SUCHOMELOVÁ, and JAN PETR

Regional Centre of Advanced Technologies and Materials, Department of Analytical Chemistry, Palacký University in Olomouc, Czech Republic
secjpetr@gmail.com

Summary

Low-cost microfluidic platforms represent an easy cheap and high-throughput alternative to modern expensive instruments. In our work, we developed a simple platform using an office laminator machine. Three types of channels were studied as a proof of a concept.

1. Introduction

A financial crisis in the world, particularly in Europe affects people's behavior, economy, competitiveness, and politics. Since this crisis seems to affect life of all the people in next years, there is a need for methods/devices/ processes that will be highly effective, competitive and cheap. The price will plays one of the most important roles and probably will be highly rated. Low-cost microfluidic platforms are known as an alternative to common instruments which have high prize and low portability. First, the title "low-cost devices" is related mainly to devices that could be developed in many copies with small costs (as PDMS chips). However, there is another possibility to lower the price by using classical filtration papers or nitrocellulose membranes as described by Whitesides et al.[1] or Yager et al.[2]. These "paper-based microfluidic devices" (μPADs) can be easily produced, modified for many purposes, and also commercialized.

In our previous works[3], we designed paper-based chips for determination of ecotoxicologically relevant heavy metals. However, we wanted to cover our chips to avoid any contact of atmosphere with the reagent zones. As described before, a simple transparent adhesive tape can be used for such purposes but this is not really reproducible approach since the tape can be easily detached. Hence, the aim of our work was to overcome problems with the transparent adhesive tape and to find more precise and reproducible approach to cover paper-chips. Recently, the similar work was presented by Cassano et al.[4] who called these devices as "laminated paper-based analytical devices" (LPADs).

2. Experimental

Paper-microfluidic devices were prepared as follows: a design was drawn using the Corel Draw X5 software; then printed by the Xerox ColorQube 8570 wax printer on filter paper Whatman, Grade 1; wax melting was done by ironing using the Tefal Primagliss 2530 iron at highest temperature (205 °C) over a bake paper. Laminating of the devices was done using automatic Fellowes Cosmic A4 laminating machine with using Fellowes Impress A4 Laminating pouches (100 μm). Next micodevices were prepared as cut paper strips (as channels) which were carefully inserted into the laminating pouch by tweezers and directly laminated. Finally, cut laminated pouches were used instead of cut paper strips to form paper-free channels, too. Microscopic observations were done by the optical microscope Motic 102M equipped with a CCD camera.

3. Results and discussion

First, we studied simple coverage of wax-printed paper-based microfluidic device by the laminating pouch. We found that the reagent zone is stable for more than 14 days and the laminating pouch prevent the chip and reagents also against e.g. low and high humidity or accidental spills onto the chips. The same results were achieved also for paper strips laminated in the pouch. The microscopic view of the laminated paper strip is in Fig. 1. As can be seen, the paper is fully covered by the laminating foil.

When the chip should be used, the laminating foil is simply cut in the place where the channel starts or a drop of analyzed liquid is placed onto the chip and the foil is

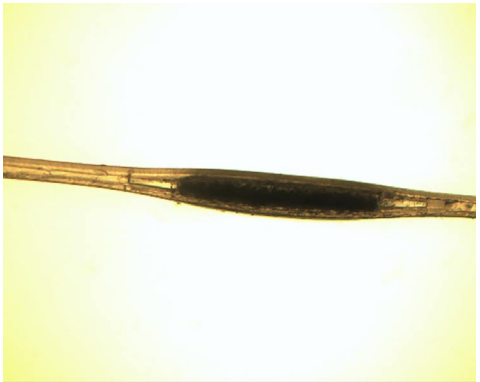

Fig. 1. **Microscopic view of the paper strip laminated in the pouch**

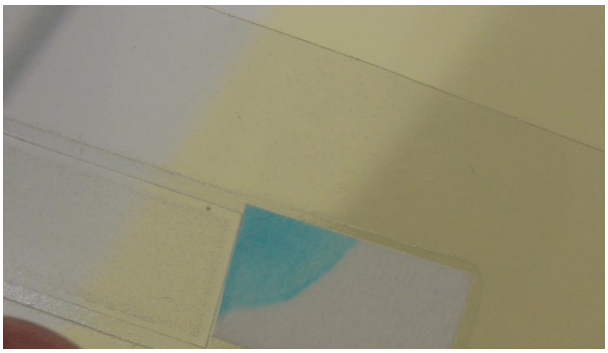

Fig. 2. **Laminated pouch-based channel with a paper-based reagent pad**

perforate by a needle. Channels in the laminating pouch can be also differently crossed allowing division of the flow or they can be bridged using a piece of parafilm between them.

Finally, a pouch laminated in advance was cut and used instead of a cut paper strip to form paper-free channels. This type of channel misses some positive effects of the paper as adhesion or partitioning but the liquid flow is much faster. Moreover, this channel can be also connected with the paper-based fluidics using paper pads as reagent zones (Fig. 2).

4. Conclusions

In this work, we designed low-cost microfluidic platforms based on the use of an office laminating machine that forms cheap and high-throughput types of analytical microdevices. We believe that our work proved the concept of using laminating pouches as covers of the chips as well as the supply for channels fabrication.

Authors gratefully acknowledge the financial support by the Operational Program Research and Development for Innovations – European Regional Development Fund (project CZ.1.05/2.1.00/03.0058) and the Operational Program Education for Competitiveness – European Social Fund (projects CZ.1.07/2.3.00/20.0018 and CZ.1.07/2.3.00/35.0023).

REFERENCES

1. Yager P., Edwards T., Fu E., Helton K., Nelson K., Tam M. R., Weigl B. H.: Nature *442*, 412 (2006).
2. Martinez A. W., Phillips S. T., Butte M. J., Whitesides G. M.: Angew. Chem. Int. Ed. *46*, 1318 (2007).
3. Petr J., Svobodová P., Vojtková L., Suchomelová A., Přibylka A., Knob R.: *MicroTAS 2013 Proceedings*, p. 1902 (2013).
4. Cassano C. L., Fan Z. H.: Microfluid. Nanofluid. *15*, 173 (2013).

THIN METAL FILMS FOR DETECTION AND PRECONCENTRATION

PAVEL PODEŠVA and FRANTIŠEK FORET

Institute of Analytical Chemistry, Brno, Czech Republic
podesva@iach.cz

Summary

Thiol specific sensor, based on measurement of the resistivity change was developed. The sensor can be regenerated many times, has a large dynamic range and its surface can be easily modified by deposition of metal nanoparticles for increased capacity.

1. Introduction

The chemiresistor is the sensor, which changes its resistivity with change of adjacent chemical environment[1,2]. In this work it is the gold thin film sensor[3] interacting with thiols in liquid phase When a thiolated molecule adsorbs on the gold surface[4,5], the covalent bond between the sulphur and gold atom is established with 50 % of C-C bond strength[6] and this effect can be represented by shift in resistance up to 5 % (ref.[7]). After washing the sensor surface, the chemisorbed thiolated compounds can be released by electric current generated by a voltage applied between the gold surface and regeneration electrode and used for further analysis. For enhancement of the retention capacity, the gold surface was modified by Au nanoparticles.

2. Experimental

2.1. Hardware

The device was constructed as a droplet plate with four circuit blocks, each with four sensing elements (spots) arranged in the Wheatstone bridge where only one element in block was used at a time when using as sensor, or as a retention column. The first metal layer was prepared by lift-off lithography and sputtering process using 3'' quartz glass. In next step was using classic lithography process for preparing a hydrophobic coating around the sensor surface. Sample was placed on the test spot by pipette in volume 25–100 μl. The sensing spots were surrounded with hydrophobic coating, keeping the drop in position.

2.2. Chemistry

To enhance the surface capacity the spot was modified by deposition of gold nanoparticles. We used the method according to ref.[8] using the well-known citrate stabilized gold colloid solution mixed with water solution of hydroquinone where 100 ml of the gold colloid was placed on each spot of the selected section, and a disc-shaped counterelectode was in contact of the top of the droplets. After applying the voltage hydroquinone was oxidized into benzoquinone producing H+ ions, canceling the charge of the citrate layer resulting in the formation of Au aggregates.

3. Results and discussion

Experiments have shown, that controlled deposition of a porous film of gold nanoparticles is possible and that the film of the Au aggregates forms much faster on the positive electrode when compared to the unconnected or negative electrode. After deposition the Au film was washed with water and baked in to decompose the remaining organics in the layer.

Financial support from the Grant Agency of the Czech Republic (P301/11/2055) and the institutional support RVO: 68081715 is acknowledged. Part of the work was realized in CEITEC – Central European Institute of Technology with research infrastructure supported by the project CZ.1.05/1.1.00/02.0068 financed from European Regional Development Fund.

Fig. 1. **Detail of the deposited layer of the gold nanoparticles (wide strips) and uncovered counterelectrode (~ 100 μm narrow strip)**

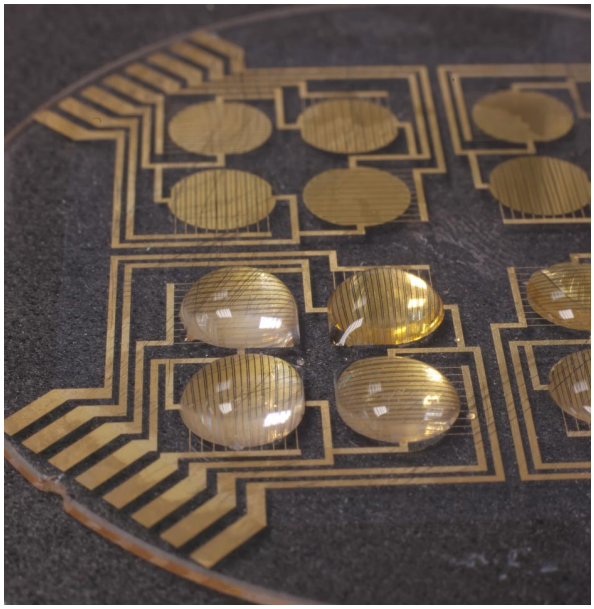

Fig. 2. **Overall view of sensor. Front section is holding droplets on spots**

REFERENCES

1. Podesva P., Foret F.: Curr. Anal. Chem. *9*, 642 (2013).
2. Tucceri R.: Surf. Sci. Rep. *56*, 85 (2004).
3. Tellier C. R.: Active and Passive Electronic Components *12*, 9 (1985).
4. Flynn N. T., Tran T. N. T., Cima M. J., Langer R.: Langmuir *19*, 10909 (2003).
5. Schonenberger C., Jorritsma J., Sondaghuethorst J. A. M., Fokkink L. G. J.: J. Phys. Chem. *99*, 3259 (1995).
6. Fried G. A., Zhang Y. M., Bohn P. W.: Thin Solid Films *401*, 171 (2001).
7. Riu J., Maroto A., Rius F. X.: Talanta *69*, 288 (2006).
8. Xu Y. Z., Zhang Y. R., Zheng J. F., Guo C., Niu Z. J., Li Z. L.: Int. J. Electrochem. Sci. *6*, 664 (2011).